

Peculiar Velocity Decomposition, Redshift Space Distortion and Velocity Reconstruction in Redshift Surveys – I. The Methodology

Pengjie Zhang,^{1,*} Jun Pan,^{2,3} and Yi Zheng¹

¹Key Laboratory for Research in Galaxies and Cosmology,
Shanghai Astronomical Observatory, Nandan Road 80, Shanghai, 200030, China

²National Astronomical Observatories, Chinese Academy of Sciences,
20A Datun Rd., Chaoyang District, Beijing 100012, P. R. China

³Purple Mountain Observatory, 2 West Beijing Rd., Nanjing 210008, P. R. China

Massive spectroscopic surveys will measure the redshift space distortion (RSD) induced by galaxy peculiar velocity to unprecedented accuracy and open a new era of precision RSD cosmology. We develop a new method to improve the RSD modeling and to carry out robust reconstruction of the 3D large scale peculiar velocity through galaxy redshift surveys, in light of RSD. (1) We propose a mathematically unique and physically motivated decomposition of peculiar velocity into three eigen-components: an irrotational component completely correlated with the underlying density field (\mathbf{v}_δ), an irrotational component uncorrelated with the density field (\mathbf{v}_S) and a rotational (curl) component (\mathbf{v}_B). The three components have different origins, different scale dependences and different impacts on RSD. (2) This decomposition has the potential to simplify and improve the RSD modeling. (I) \mathbf{v}_B damps the redshift space clustering. (II) \mathbf{v}_S causes both damping and enhancement to the redshift space power spectrum $P^s(k, u)$. Nevertheless, the leading order contribution to the enhancement has a u^4 directional dependence, distinctively different to the Kaiser formula. Here, $u \equiv k_z/k$, k is the amplitude of the wavevector and k_z is the component along the line of sight. (III) \mathbf{v}_δ is of the greatest importance for the RSD cosmology. We find that the induced redshift clustering shows a number of important deviations from the usual Kaiser formula. Even in the limit of $\mathbf{v}_S \rightarrow 0$ and $\mathbf{v}_B \rightarrow 0$, the leading order contribution $\propto (1 + f\tilde{W}(k)u^2)^2$. It differs from the Kaiser formula by a window function $\tilde{W}(k)$. Nonlinear evolution generically drives $\tilde{W}(k) \leq 1$. We hence identify a significant systematical error causing underestimation of the structure growth parameter f by as much as $O(10\%)$ even at relatively large scale $k = 0.1h/\text{Mpc}$. (IV) The velocity decomposition reveals the three origins of the finger of God (FOG) effect and suggests to simplify and improve the modeling of FOG by treating the three components separately. (V) We derive a new formula for the redshift space power spectrum. Under the velocity decomposition scheme, all high order Gaussian corrections and non-Gaussian correction of order δ^3 can be taken into account *without introducing extra model uncertainties*. Here δ is the nonlinear overdensity. (3) The velocity decomposition clarifies issues in peculiar velocity reconstruction through 3D galaxy distribution. We discuss two possible ways to carry out the 3D \mathbf{v}_δ reconstruction. Both use the otherwise troublesome RSD in velocity reconstruction as a valuable source of information. Both have the advantage to render the reconstruction of a stochastic 3D field into the reconstruction of a deterministic window function $W^s(k, u)$ of limited degrees of freedom. Both can automatically and significantly alleviate the galaxy bias problem and, in the limit of a deterministic galaxy bias, completely overcome it. Paper I of this series of works lays out the methodology. Companion papers [1] will extensively evaluate its performance against N-body simulations.

PACS numbers: 98.80.-k; 98.80.Es; 98.80.Bp; 95.36.+x

I. INTRODUCTION

The observed galaxy clustering pattern in redshift space is modified by peculiar velocity of galaxies and shows characteristic anisotropies [2–7]. This redshift space distortion (RSD) effect provides a promising way to measure peculiar velocity at cosmological distance and makes itself a powerful probe of the dark universe. It has allowed the measurement of the structure growth rate in spectroscopic surveys such as 2dF [8, 9], SDSS [10, 11], VVDS [12], WiggleZ [13, 14] and BOSS [15, 16]. Such

growth rate measurement is highly valuable in probing the nature of dark energy [17–24] and gravity [25–32]. In particular, with both the expansion rate measurement from BAO [33–36] and structure growth rate measurement from RSD, spectroscopic redshift surveys are well suited to test consistency relations in general relativity and to discriminate between dark energy and modified gravity [37]. For these reasons, RSD has become one of the key science goals of the planned stage IV dark energy projects such as the BigBOSS experiment [38] and the Euclid cosmology mission [39]. It can also be used to measure the stochastic galaxy bias [40] and the galaxy (pairwise) velocity dispersion [41], both are valuable for studying galaxy formation.

These applications heavily relies on the RSD modeling. However, modeling RSD to accuracy matching stage

*Email me at: pjzhang@shao.ac.cn

IV dark energy projects is very challenging, especially due to three sources of nonlinear and the associated non-Gaussianity. (1) The nonlinear mapping from real space clustering to redshift space clustering. Due to this nonlinearity, even the lowest order statistics in redshift space involves correlations between density and velocity fields to infinite order (e.g. [42–45]). (2) The nonlinear evolution in the real space matter density and velocity fields. (3) The nonlinear and nonlocal galaxy-matter relation. The galaxy density bias is known to have non-negligible nonlinearity and stochasticity (e.g. [46]). The galaxy velocity bias may also be needed for precision modeling (e.g. [47]). To proceed, layers of approximations and simplifications have been made.

Here we elaborate on some of these approximations/simplifications with example of matter clustering in redshift space. One of the most commonly used RSD formulae connecting the isotropic real space power spectrum $P_{\delta\delta}(k)$ to the anisotropic redshift space power spectrum $P_{\delta\delta}^s(k, u)$ is $P_{\delta\delta}^s(k, u) \simeq P_{\delta\delta}(k)(1 + fu^2)^2 D^{\text{FOG}}(ku)$. It is a phenomenological combination and extension of the linear Kaiser effect and the finger of God (FOG) effect due to random motions. Here, $f \equiv d \ln D / d \ln a$ and $D \equiv D(z)$ is the linear density growth factor at redshift $z = 1/a - 1$. Throughout this paper, the superscript “s” denotes the property in redshift space. $P_{\delta\delta}^s$ depends on both k and $u \equiv k_{\parallel}/k$. Throughout the paper we adopt the z -axis as the line of sight, so $k_{\parallel} = k_z$. Approximations/simplifications made include (1) the parallel plane approximation [48], (2) linear evolution in the velocity-density relation and (3) no stochasticity between the velocity and density field [22]. (4) It also neglects most high order correlations between the density and velocity fields [43, 44]. (5) $D^{\text{FOG}}(ku)$ is a phenomenological description of the FOG effect, the overall damping caused by random motion. Both a Gaussian form $D^{\text{FOG}}(ku) = \exp(-(ku\sigma_v/H)^2)$ and a Lorentz form $D^{\text{FOG}}(ku) = 1/(1 + (ku\sigma_P/H)^2/2)$ are widely adopted. However, the physical meaning of the velocity dispersion σ_v and especially the pairwise velocity dispersion σ_P is a bit ambiguous. Furthermore, deviations from the above forms have been found in simulations [49].

Various approaches have been investigated to improve the RSD modeling. A far from complete list includes the Eulerian and Lagrangian perturbation theory [42, 47, 50–56], the halo model [49, 57–60], the streaming model [4, 61, 62], the recently proposed distribution function approach [43–45] and combinations between them. Furthermore, due to significant nonlinearities involved, RSD modeling often resorts to numerical simulations on calibration and testing (e.g. [42, 49, 59, 62–65]). Despite these efforts, RSD modeling has not yet achieved the accuracy required for precision RSD cosmology. For example, recent tests against N-body simulations find that the inferred f can be biased low by $O(10\%)$ or more [63–68], significantly larger than the $O(1\%)$ statistical error in f for surveys like BigBOSS and Euclid.

Since RSD is induced by peculiar velocity, it is of cru-

cial importance to understand the peculiar velocity field. We find that, an appropriate velocity decomposition has the potential to simplify and improve the RSD modeling. We also find that the same decomposition may enable robust reconstruction of 3D peculiar velocity in spectroscopic surveys. It has the advantage to render the otherwise troublesome RSD in velocity reconstruction into valuable source of information. The current paper aims to lay out the methodology of the proposed velocity decomposition, RSD modeling and 3D velocity reconstruction. Extensive tests against simulations and mock catalogs are required to clarify/justify/quantify numerous technical issues. These numerical results will be presented in companion papers [1].

This paper is organized as follows. In §II we decompose the peculiar velocity fields into three eigen-modes (\mathbf{v}_δ , \mathbf{v}_S and \mathbf{v}_B) and discuss related statistics. Among them, \mathbf{v}_δ is the velocity component completely correlated with the density distribution and is the one contains most cosmological information. In §III we show that the three velocity components affect RSD in different ways and their impacts can be treated separately. We are then able to derive the exact RSD formula. Furthermore we propose reasonable approximations for realistic calculation. Through this methodology, we explicitly identify a significant systematical error in RSD cosmology. §IV proposes a method to reconstruct the 3D \mathbf{v}_δ from redshift surveys and the appendix D proposes an alternative. For brevity, the above sections focus on the matter field. But these results can be extended to the galaxy field straightforwardly, as briefly discussed in §V. We further argue that the velocity reconstruction is insensitive to the galaxy bias. At the end of each sections, we list key statistics to be investigated in future works. We also prepare four appendices for more technical issues.

II. PECULIAR VELOCITY DECOMPOSITION

Any vector field can be decomposed into a irrotational (gradient) part and a rotational (curl) part. Analogous to the electric and magnetic fields (and also the CMB polarization field and the cosmic shear field), we denote the first one with a subscript “E” and the later one with a subscript “B”. Hence the peculiar velocity \mathbf{v} can be decomposed as

$$\mathbf{v}(\mathbf{x}) = \mathbf{v}_E(\mathbf{x}) + \mathbf{v}_B(\mathbf{x}) . \quad (1)$$

By definition, $\nabla \times \mathbf{v}_E = 0$ and $\nabla \cdot \mathbf{v}_B = 0$. In Fourier space, we have $\mathbf{v}_E(\mathbf{k}) = [\mathbf{v}(\mathbf{k}) \cdot \hat{\mathbf{k}}]\hat{\mathbf{k}}$ and $\mathbf{v}_B(\mathbf{k}) = \mathbf{v}(\mathbf{k}) - \mathbf{v}_E(\mathbf{k})$.

\mathbf{v}_E can be completely described by its divergence $\theta(\mathbf{x}) \equiv -\nabla \cdot \mathbf{v}(\mathbf{x})/H \equiv -\nabla \cdot \mathbf{v}_E(\mathbf{x})/H$. To conveniently describe the velocity-density relation, we carry out a further decomposition,

$$\mathbf{v}_E(\mathbf{x}) = \mathbf{v}_\delta(\mathbf{x}) + \mathbf{v}_S(\mathbf{x}) . \quad (2)$$

Both \mathbf{v}_δ and \mathbf{v}_S are irrotational ($\nabla \times \mathbf{v}_\delta = 0$ and $\nabla \times \mathbf{v}_S = 0$). We require that $\theta_\delta \equiv -\nabla \cdot \mathbf{v}_\delta/H$ is completely correlated with the overdensity δ . So we denote this component with a subscript “ δ ”. In Fourier space, we then have

$$\theta_\delta(\mathbf{k}) = \delta(\mathbf{k})W(\mathbf{k}). \quad (3)$$

Here $W(\mathbf{k})$ is a deterministic function of \mathbf{k} to be determined later.

On the other hand, we require that $\theta_S \equiv -\nabla \cdot \mathbf{v}_S/H$ is uncorrelated with δ . So $\langle \theta_S(\mathbf{x})\delta(\mathbf{x} + \mathbf{r}) \rangle = 0$. Equivalently $\langle \theta_S(\mathbf{k}')\delta(\mathbf{k}) \rangle = 0$ for any \mathbf{k} and \mathbf{k}' . θ_S is the source of stochasticity in the δ - θ relation, so we denote this component with a subscript “ S ”.

We define the power spectrum between field A and field B through $\langle A(\mathbf{k})B(\mathbf{k}') \rangle \equiv (2\pi)^3 \delta_{3D}(\mathbf{k} + \mathbf{k}') P_{AB}(\mathbf{k})$. We often use the notation $\Delta_{AB}^2 \equiv k^3 P_{AB}/(2\pi^2)$, which enters into the ensemble average $\langle A(\mathbf{x})B(\mathbf{x}) \rangle = \int \Delta_{AB}^2(k) dk/k$. Through the relation $\langle \delta(\mathbf{k}')\theta(\mathbf{k}) \rangle = \langle \delta(\mathbf{k}')\theta_\delta(\mathbf{k}) \rangle = \langle \delta(\mathbf{k}')\delta(\mathbf{k}) \rangle W(\mathbf{k})$, we obtain

$$W(\mathbf{k}) = W(k) = \frac{P_{\delta\theta}(k)}{P_{\delta\delta}(k)}. \quad (4)$$

Notice that, due to the isotropy of the universe, $P_{\delta\theta}(\mathbf{k}) = P_{\delta\theta}(k)$ and $P_{\delta\delta}(\mathbf{k}) = P_{\delta\delta}(k)$. So W does not depend on the direction of \mathbf{k} .

Hence we prove that the velocity decomposition into \mathbf{v}_δ , \mathbf{v}_S and \mathbf{v}_B is mathematically unique, with no assumptions on the underlying density and velocity field. But the decomposition has strong physical motivation too. The three components are associated with different physical processes in the structure formation. We now proceed to their physical meanings.

A. The \mathbf{v}_δ field

In the limit $k \ll k_{\text{NL}}$, \mathbf{v}_δ is the only velocity component. Here k_{NL} is the nonlinear scale, defined through $\Delta_{\delta\delta}^2(k_{\text{NL}}) = 1$. \mathbf{v}_B is a decay mode before shell crossing so it is negligible in the linear regime [69, 70]. On the other hand, in the limit $k \ll k_{\text{NL}}$, \mathbf{v}_E is completely correlated with the density field, with a deterministic relation $\theta = f\delta$. So \mathbf{v}_S vanishes too. \mathbf{v}_δ , being the most linear velocity component, is of the greatest interest to cosmology.

Nevertheless, nonlinear evolution leaves non-negligible imprints in the \mathbf{v}_δ field. A crucial point is that nonlinear evolution affects the density field and the velocity field in different or even opposite ways (e.g. [42, 69]). The third order Eulerian perturbation theory shows that, when the effective power index $n_{\text{eff}} \gtrsim -1.9$, nonlinear evolution actually suppresses the velocity growth, while enhances the overdensity growth (Fig. 12, [69]). Even for $n_{\text{eff}} \lesssim -1.9$, θ grows more slowly than the overdensity (Fig. 12, [69]). Furthermore, nonlinear evolution generates a

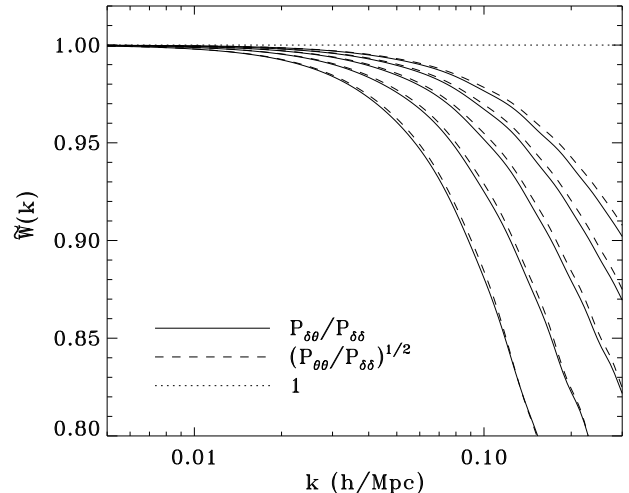


FIG. 1: Solid lines are $\tilde{W}(k, z)$ predicted by the third order Eulerian perturbation theory at redshift $z = 0.0, 0.5, 1.0, 1.5, 2.0$ (bottom up). We adopt a flat Λ CDM cosmology with $\Omega_m = 0.26$, $\Omega_b = 0.044$, $\Omega_\Lambda = 0.74$, $h = 0.71$, $\sigma_8 = 0.8$ and $n_s = 1$. Nonlinearity drives \tilde{W} down from unity. Later we will show that what inferred from redshift space distortion is $f\tilde{W}$. So the structure growth rate f can be biased low by $O(10\%)$, consistent with recent findings (e.g. [63–68]). To demonstrate the \mathbf{v}_S component, we also plot $\sqrt{P_{\theta\theta}/P_{\delta\delta}}$, normalized to unity at $k \rightarrow 0$ (dash lines). $\sqrt{P_{\theta\theta}/P_{\delta\delta}} = P_{\delta\theta}/P_{\delta\delta} \times \sqrt{1+\eta}$. $\eta \equiv P_{\theta_S\theta_S}/P_{\theta_\delta\theta_\delta}$ quantifies the relative amplitude of \mathbf{v}_S with respect to the velocity component \mathbf{v}_δ . It also quantifies the velocity divergence-density stochasticity (Eq. 7). In the limit $k \rightarrow 0$, $\eta \rightarrow 0$ and $\sqrt{P_{\theta\theta}/P_{\delta\delta}} \rightarrow P_{\delta\theta}/P_{\delta\delta}$. The nonlinear evolution generates \mathbf{v}_S and causes the two sets of curves to deviate from each other. Since the third order Eulerian perturbation theory has limited range of applicability, numerical results shown in this plot are mainly presented to demonstrate the major impacts of the nonlinear evolution such as driving \tilde{W} down from unity and driving η up from zero. Robust quantifications of \tilde{W} and η will be presented in companion papers [1].

stochastic velocity component \mathbf{v}_S , further reducing θ_δ with respect to δ . In the deeply nonlinear regime, after many orbit crossings, the velocity field eventually loses its correlation with the density field and we expect $\mathbf{v}_\delta \rightarrow 0$.

Hence we should use Eq. 4 to describe the θ_δ - δ relation, instead of the linear relation $\theta_\delta = f\delta$. For the convenience of highlighting the deviation from the linear relation, we define the normalized \tilde{W} through

$$\tilde{W}(k) \equiv \frac{W(k)}{W(k \rightarrow 0)} = \frac{W(k)}{f} = \frac{1}{f} \frac{P_{\delta\theta}(k)}{P_{\delta\delta}(k)}. \quad (5)$$

\tilde{W} calculated using the third order Eulerian perturbation theory is shown in Fig. 1. In companion papers [1] we will numerically evaluate this key quantity using high resolution N-body simulations. In the limit $k \rightarrow 0$, $\tilde{W} \rightarrow 1$ as expected. But nonlinear evolution soon drives

\tilde{W} to deviate $\tilde{W} < 1$. Even at relatively high redshift $z = 2$ and pretty linear scale $k = 0.1h/\text{Mpc}$, the deviation already reaches $O(1\%)$. The derivation increases towards low redshift and exceeds 10% at $z \lesssim 0.5$.

To better understand this behavior, we can express \tilde{W} as

$$\tilde{W}(k) = r_{\delta\theta}(k) \sqrt{\frac{P_{\theta\theta}(k)}{f^2 P_{\delta\delta}(k)}} \leq \sqrt{\frac{P_{\theta\theta}(k)}{f^2 P_{\delta\delta}(k)}} \leq 1. \quad (6)$$

Here, $r_{\delta\theta}(k)$ is the cross correlation coefficient between δ and θ . By definition, $r_{\delta\theta}(k) \leq 1$. Given the fact that velocity grows more slowly than the density, $P_{\theta\theta} < f^2 P_{\delta\delta}$. So we expect $\tilde{W} < 1$ in nonlinear regime. Furthermore, when $k \gg k_{\text{NL}}$, $r_{\delta\theta} \rightarrow 0$. So we expect $\tilde{W} \rightarrow 0$ when $k \gg k_{\text{NL}}$.

The recognition of the velocity component \mathbf{v}_δ has several important applications. (1) It lays out a promising way to reconstruct the 3D peculiar velocity from 3D density distribution, which is accessible from galaxy spectroscopic redshift surveys. \tilde{W} mimics a window function with a smoothing scale comparable to the nonlinear scale. It exerts on the density field and suppresses small scale inhomogeneities so that the smoothed density field provides a honest estimation on the underlying velocity field \mathbf{v}_δ . One can find a similar window function exerting on the redshift space density, which is directly observable. Hence the reconstruction of the stochastic 3D vector field is simplified to the reconstruction of a deterministic window function with limited degrees of freedom. This is one of the most important applications of the velocity decomposition proposed in this paper. Later in §IV we will present more detailed investigation. (2) It simplifies the RSD modeling. Since $\tilde{W} \rightarrow 0$ toward small scales, nonlinearity and non-Gaussianity in the \mathbf{v}_δ field are significantly suppressed. (3) It identifies a severe systematical error in RSD cosmology. Later in §III C we will show that RSD is determined by $f\tilde{W}$ instead of f . If the factor \tilde{W} is not included in the RSD cosmology, f will be biased low by $\sim 2\%$ at $z = 2$ and $\sim 10\%$ at $z = 0$, even if we restrict the analysis to $k \lesssim 0.1h/\text{Mpc}$. To our best knowledge, this is the first time such systematical error could explain recent findings of $O(10\%)$ underestimation in f inferred from simulated RSD data [63–68]. We will present more discussions on its cosmological implications in §III E.

B. The \mathbf{v}_S field

To the opposite of \mathbf{v}_δ , \mathbf{v}_S vanishes in the linear regime and begins to grow due to the nonlinear evolution. For this reason, it lacks large scale power and hence its correlation length is smaller than that of \mathbf{v}_δ . For the same reason, it is intrinsically non-Gaussian. Being uncorrelated to the density field, \mathbf{v}_S induce stochasticities in the

velocity-density relation. We have the relation

$$r_{\delta\theta}(k) \equiv \frac{P_{\delta\theta}(k)}{\sqrt{P_{\delta\delta}(k)P_{\theta\theta}(k)}} = \frac{1}{\sqrt{1 + \eta(k)}}, \quad (7)$$

where $\eta(k) \equiv P_{\theta_S\theta_S}(k)/P_{\theta_S\theta_S}(k)$. When \mathbf{v}_S overwhelms over \mathbf{v}_δ ($\eta \gg 1$), $r_{\delta\theta} \rightarrow 0$ and the velocity field loses its correlation with the density field.

Based on the third order perturbation calculation, we find that $P_{\theta_S\theta_S}$ already reaches $\simeq 1\%$ of $P_{\theta_S\theta_S}$ (namely $\eta \simeq 1\%$) at $k = 0.1h/\text{Mpc}$ and $z \lesssim 1$, as can be inferred from Fig. 1. As expected, the situation is less severe at higher redshifts. But even at $z = 2$, $\eta \simeq 1\%$ at $k = 0.2h/\text{Mpc}$. Hence in general, \mathbf{v}_S is a non-negligible velocity component even at scales which are often considered as linear. Nevertheless, it is still subdominant to \mathbf{v}_δ at scale $k \lesssim 1h/\text{Mpc}$, as one can infer from Fig. 1 of [22], in combination with our Eq. 7. Our numerical evaluations obtain similar results [1].

What cosmological information does \mathbf{v}_S contain? One particularly interesting piece of information is likely the nature of gravity. For modified gravity models to pass the solar system tests and to drive the late time cosmic acceleration, gravity must behave upon the environment (e.g. review articles [71, 72]). Such environmental dependence often becomes prominent in the nonlinear regime, so it can significantly affect the velocity divergence (e.g. [32]). Arisen from nonlinear evolution, \mathbf{v}_S would be sensitive to this generic feature of modified gravity, making it attractive for testing gravity.

In §III we will show that the \mathbf{v}_S induced RSD differs from the \mathbf{v}_δ induced RSD (§III). We argue that these differences can be used to separate the different velocity components and to make *statistical* measurement of \mathbf{v}_S possible.

C. The \mathbf{v}_B field

\mathbf{v}_B decays as long as the single fluid approximation for the dark matter distribution holds [69]. \mathbf{v}_B grows only when the nonlinearity is sufficiently large that shell crossing happens. In the deeply nonlinear regime, we may even expect equi-partition in the velocity distribution and \mathbf{v}_B can dominate over \mathbf{v}_E . So we expect that its power concentrates at even smaller scales than \mathbf{v}_S . Indeed, numerical studies [70] show that the power of this velocity component concentrates at small scales, with r.m.s. much smaller than that of \mathbf{v}_E . Our numerical evaluations found similar behavior [1]. Later in §III A we will show that these behaviors significantly simplify the modeling of \mathbf{v}_B induced RSD. We refer the readers to [70] and references therein for in depth study of \mathbf{v}_B . In [1], we will present our numerical evaluations on RSD related statistics of \mathbf{v}_B .

D. Statistical description of the three velocity components

This paper is not at a position to calculate the statistics of these velocity components. Instead, we present some general discussions here and postpone any quantitative calculations into future works. First, since the three velocity components have different origins, the halo model scenario [41, 73–75] provides an unified way to describe the three components. Nevertheless, a number of extensions/corrections may be necessary. (1) Since the linear perturbation theory fails to describe the emergence of \mathbf{v}_S and deviations from the linear theory prediction of the halo bulk motion have been diagnosed [76], a natural extension to describe the halo bulk motion is the third order perturbation. (2) Peculiar velocity has been treated as the sum of the halo bulk velocity and the random velocity inside of the virialized halos [77]. It may be extended to include the more complicated motion around the halo outskirts, which may be a significant source of \mathbf{v}_B [70]. Nevertheless, treatment of \mathbf{v}_B is trickier and we refer the readers to [70] for detailed discussions.

One important statistics relevant to RSD is the velocity correlation function. Due to symmetry considerations, it can be decomposed as [4]

$$\langle v_i(\mathbf{x}_1)v_j(\mathbf{x}_2) \rangle = \psi_{\perp}(r)\delta_{ij} + [\psi_{\parallel}(r) - \psi_{\perp}(r)] \frac{r_i r_j}{r^2}. \quad (8)$$

Here $\mathbf{r} \equiv \mathbf{x}_1 - \mathbf{x}_2$ is the pair separation vector and $i = x, y, z$ is the Cartesian axes. ψ_{\parallel} is the correlation function when both v_i and v_j are along \mathbf{r} . ψ_{\perp} is the one when both velocities are perpendicular to \mathbf{r} .

ψ_{\parallel} and ψ_{\perp} are not independent. For a potential flow (\mathbf{v}_{δ} and \mathbf{v}_S), we have the textbook result [4]

$$\psi_{\parallel}(r) = \frac{d(r\psi_{\perp}(r))}{dr}, \quad (9)$$

$$\psi_{\perp}(r) = H^2 \int \Delta_{\theta\theta}^2 \frac{\sin(kr)}{kr} \frac{dk}{k^3}. \quad (10)$$

Here we have defined the velocity power spectrum through $\langle \mathbf{v}(\mathbf{k}) \cdot \mathbf{v}(\mathbf{k}') \rangle \equiv (2\pi)^3 \delta_{3D}(\mathbf{k} + \mathbf{k}') P_{vv}(k)$. Its covariance is defined as $\Delta_{vv}^2 \equiv P_{vv} k^3 / 2\pi^2$.

On the other hand, \mathbf{v}_B does not follow this relation. Using the fact that \mathbf{v}_B can be expressed as the vorticity of a vector \mathbf{A} ($\mathbf{v}_B = \nabla \times \mathbf{A}$), we derive the following relations,

$$\psi_{\perp}(r) = \psi_{\parallel}(r) + \frac{1}{2} r \frac{d\psi_{\parallel}(r)}{dr}, \quad (11)$$

$$\psi_{\parallel}(r) = \int \Delta_{v_B v_B}^2(k) \frac{dk}{k} \frac{1}{3} \left[\frac{\sin kr}{(kr)^3} - \frac{\cos kr}{(kr)^2} \right]. \quad (12)$$

E. To do list

In companion papers [1], we will use N-body simulations to numerically evaluate statistics of these velocity fields. An incomplete list includes

- The power spectra $P_{v_{\delta}v_{\delta}}(k, z)$, $P_{v_S v_S}(k, z)$ and $P_{v_B v_B}(k, z)$. Their scale and redshift dependences are helpful to understand the impact of nonlinear evolution.
- The correlation function $\psi_{v_{\delta}v_{\delta}}(r, z)$, $\psi_{v_S v_S}(r, z)$ and $\psi_{v_B v_B}(r, z)$, of the “ \parallel ” mode and the “ \perp ” mode. These statistics quantify the correlation length of the three velocity components and tell us at which separation we can treat the velocities at two positions as independent.
- The PDFs of \mathbf{v}_{δ} , \mathbf{v}_S and \mathbf{v}_B . The PDFs determine the overall damping (FOG) to the redshift power spectrum. We will also calculate the cumulants to quantify non-Gaussianity of these velocity components.
- $\tilde{W}(k, z)$. As we have addressed, \tilde{W} is of crucial importance in the 3D velocity reconstruction and in the RSD cosmology. Through N-body simulations, we will robustly measure its dependence on k and z . Furthermore, we want to quantify the $\tilde{W}(k, z)$ - $\Delta_{\delta\delta}^2(k, z)$ relation to better understand its dependence on the nonlinearity. Especially, we want to know if it can be well approximated by a simple function with only a few parameters.

III. MODELING THE REDSHIFT SPACE DISTORTION

Now we proceed to the RSD modeling with the aid of the proposed velocity decomposition. Following [42], we utilize the matter conservation ($(1 + \delta^s(\mathbf{x}^s))d^3\mathbf{x}^s = (1 + \delta(\mathbf{x}))d^3\mathbf{x}$) to derive

$$\delta^s(\mathbf{k}) = \int [1 + \delta(\mathbf{x})] \exp\left(i \frac{k_z v_z}{H}\right) \exp(i\mathbf{k} \cdot \mathbf{x}) d^3\mathbf{x} \quad (13)$$

In the above expression, we have neglected a Dirac function which only shows up when $\mathbf{k} = 0$, irrelevant to our calculation. This equation adopts the plane parallel approximation and adopts the line of sight as the z -axis. It also assumes no multiple streaming. Extension to this more complicated situation can be done by the phase space distribution function approach [43–45]. Phenomenologically speaking, multiple streaming can be described by an overall damping to the redshift space power spectrum. Hence we do not expect major changes to the results presented in this paper.

The redshift space power spectrum is given by [42]

$$P_{\delta\delta}^s(\mathbf{k}) = \int \langle (1 + \delta_1)(1 + \delta_2) \exp \lambda \rangle \exp(-i\mathbf{k} \cdot \mathbf{r}) d^3\mathbf{r} \quad (14)$$

where $\delta_i \equiv \delta(\mathbf{x}_i)$ and $\mathbf{x}_2 \equiv \mathbf{x}_1 + \mathbf{r}$. The ensemble average $\langle \dots \rangle$ is averaged over all \mathbf{x}_1 with fixed \mathbf{r} . For brevity, we have denoted $\lambda \equiv ik_z(v_{1z} - v_{2z})/H$. We also denote $\lambda_{\alpha} \equiv ik_z(v_{1z,\alpha} - v_{2z,\alpha})/H$ where $\alpha = \delta, S, B$. Due to the axial

symmetry along the line of sight, $P_{\delta\delta}^s(\mathbf{k})$ only depends on k and u . Hereafter we often write it as $P_{\delta\delta}^s(k, u)$.

An immediate result is that $\delta^s(\mathbf{k}_\perp, k_z = 0) = \delta(\mathbf{k}_\perp, k_z = 0)$ and $P_{\delta\delta}^s(\mathbf{k}_\perp, k_z = 0) = P_{\delta\delta}^s(k_\perp)$. A similar relation holds for the bispectrum, $B_3^s(\mathbf{k}_1, \mathbf{k}_2, \mathbf{k}_3) = B_3(\mathbf{k}_1, \mathbf{k}_2, \mathbf{k}_3)$ when $k_{1,z} = k_{2,z} = k_{3,z} = 0$. Later we will show that these relations are very useful in RSD modeling. Notice that no such relations exist in real space. For example, $\xi^s(\mathbf{r}_\perp, r_z = 0) \neq \xi(r_\perp)$.

A. The role of \mathbf{v}_B

Now we will apply the velocity decomposition to Eq. 14. Since only \mathbf{v}_δ is correlated with the overdensity, Eq. 14 can be reduced to

$$P_{\delta\delta}^s(k, u) = \int \{ \langle (1 + \delta_1)(1 + \delta_2) \exp \lambda_\delta \rangle \times D_S(k_z, \mathbf{r}) D_B(k_z, \mathbf{r}) \} \exp(-i\mathbf{k} \cdot \mathbf{r}) d^3\mathbf{r} . \quad (15)$$

The two function $D_S(k_z, \mathbf{r})$ and $D_B(k_z, \mathbf{r})$ completely describe the redshift distortion caused by \mathbf{v}_S and \mathbf{v}_B respectively.

$$D_S(k_z, \mathbf{r}) \equiv \left\langle \exp \left(i \frac{k_z (v_{1z,R} - v_{2z,R})}{H} \right) \right\rangle , \quad (16)$$

$$D_B(k_z, \mathbf{r}) \equiv \left\langle \exp \left(i \frac{k_z (v_{1z,B} - v_{2z,B})}{H} \right) \right\rangle . \quad (17)$$

Due to the symmetry between k_z and $-k_z$, $D_{S,B}(k_z, \mathbf{r}) = D_{S,B}(|k_z|, \mathbf{r})$.

We have $D_S \leq 1$ and $D_B \leq 1$, so both \mathbf{v}_S and \mathbf{v}_B suppress the clustering presented by terms inside of the bracket of Eq. 15. However, \mathbf{v}_S and \mathbf{v}_B can have their own clusterings and hence can in principle increase the overall clustering in redshift space. We can also define a corresponding function for \mathbf{v}_δ ,

$$D_\delta(k_z, \mathbf{r}) \equiv \left\langle \exp \left(i \frac{k_z (v_{1z,\delta} - v_{2z,\delta})}{H} \right) \right\rangle . \quad (18)$$

But since \mathbf{v}_δ is correlated with the density field, its role in RSD is too complicated to be described by a single function D_δ .

In general, these functions depend on the pair separation \mathbf{r} , due to correlations in the corresponding velocity fields. To describe this effect, we define

$$1 + \epsilon_\alpha(\mathbf{r}, k_z) \equiv \frac{D_\alpha(k_z, \mathbf{r})}{D_\alpha(k_z, r \rightarrow \infty)} . \quad (19)$$

Here, $\alpha = \delta, S, B$ respectively. The limit $r \rightarrow \infty$ corresponds to the limit of no velocity correlation. In this limit, peculiar velocity only causes damping (FOG). Hence we denote D at this limit with a superscript ‘‘FOG’’,

$$D_\alpha(k_z, r \rightarrow \infty) \equiv D_\alpha^{\text{FOG}}(k_z) = \left| \left\langle \exp \left(i \frac{k_z v_{z,\alpha}}{H} \right) \right\rangle \right|^2 . \quad (20)$$

As discussed in §II, \mathbf{v}_B arises mostly in the deeply non-linear regime, so we expect a correlation length shorter than scales of interest for RSD cosmology. Hence we can neglect correlation in the \mathbf{v}_B field. Namely, we can make the approximation

$$\epsilon_B \simeq 0 \quad , \quad D_B(k_z, \mathbf{r}) \simeq D_B^{\text{FOG}}(k_z) . \quad (21)$$

Since D_B^{FOG} is independent of \mathbf{r} , Eq. 15 is simplified as

$$P_{\delta\delta}^s(k, u) = \left\{ \int \langle (1 + \delta_1)(1 + \delta_2) \exp \lambda_\delta \rangle D_S(k_z, \mathbf{r}) \exp(-i\mathbf{k} \cdot \mathbf{r}) d^3\mathbf{r} \right\} D_B^{\text{FOG}}(k_z) . \quad (22)$$

The damping function D_B^{FOG} is related to its velocity PDF through

$$\begin{aligned} \sqrt{D_B^{\text{FOG}}(k_z)} &= \int_{-\infty}^{\infty} \exp \left(i \frac{k_z v_{z,B}}{H} \right) P_B(v_{z,B}) dv_{z,B} \\ &= \int_{-\infty}^{\infty} \cos \left(\frac{k_z v_{z,B}}{H} \right) P_B(v_{z,B}) dv_{z,B} . \end{aligned}$$

Through the cumulant expansion theorem, we can express D_B^{FOG} in cumulants of $v_{z,B}$. The cumulant expansion theorem states that

$$\begin{aligned} \left\langle \exp \left(i \frac{k_z v}{H} \right) \right\rangle &= \exp \left(\sum_{n=1}^{\infty} \left(\frac{ik_z}{H} \right)^n \frac{\langle v^n \rangle_c}{n!} \right) \\ &= \exp \left(-\frac{k_z^2 \sigma_v^2}{2H^2} \right) \exp \left(\sum_{j \geq 2} (-1)^j \left(\frac{k_z \sigma_v}{H} \right)^{2j} \frac{K_{2j}}{(2j)!} \right) \\ &= \exp \left(-\frac{x}{2} \left[1 - \frac{K_4}{12} x + \frac{K_6}{360} x^2 + \dots \right] \right) . \end{aligned} \quad (23)$$

Here, v denotes $v_{z,B}$. $\langle \dots \rangle_c$ is the corresponding cumulant of the quantity inside of the bracket. For a Gaussian velocity distribution, we have $\langle v^j \rangle_c = 0$ for $j \geq 3$ and recover the Gaussian FOG. For non-Gaussian distribution, higher order terms show up. Since $\langle v^{2j+1} \rangle_c = 0$, only even cumulants contribute. $K_j \equiv \langle v^j \rangle_c / \sigma_v^j$ is the reduced cumulant and $x \equiv (k_z \sigma_v / H)^2$.

Non-Gaussianity in \mathbf{v}_B could be significant and we may expect that high order cumulants must be included to robustly model D_B^{FOG} . Fortunately, the reality can be much simpler due to the fact that \mathbf{v}_B has a σ_v much smaller than that of \mathbf{v}_E [1, 70]. Hence for the scales of interest (e.g. $k < 1h/\text{Mpc}$), we have $x \ll 1$. Then the \mathbf{v}_B induced FOG can be well described by the following Gaussian form,

$$D_B^{\text{FOG}}(k_z) \simeq \exp \left(-\frac{k_z^2 \sigma_{v_B}^2}{H^2} \right) . \quad (24)$$

σ_{v_B} is hard to calculate from first principle, so it shall be treated as a free parameter to be fitted by the data.

B. The role of \mathbf{v}_S

The situation for \mathbf{v}_S is more complicated. Since a significant fraction of \mathbf{v}_S comes from bulk motion, \mathbf{v}_S can be still correlated over $O(10)$ Mpc separation. So we are no longer able to make the approximation $\epsilon_S = 0$. Instead, we have, with the aid of the cumulant expansion theorem,

$$1 + \epsilon_S(\mathbf{r}, k_z) = \exp \left[\frac{k_z^2 \langle v_{1z,S} v_{2z,S} \rangle}{H^2} \right] \quad (25)$$

$$\times e^{[k_z^4 (3v_{1z,S}^2 v_{2z,S}^2 - 2(v_{1z,S}^3 v_{2z,S} + 1 \leftrightarrow 2))_c / 12H^4 + \dots]}$$

$$= 1 + \frac{k_z^2 \langle v_{1z,S} v_{2z,S} \rangle}{H^2} + O(v_S^4).$$

Due to the symmetry $v \leftrightarrow -v$, odd terms in v do not show up in the above equation. Plugging it into Eq. 22, we find that the leading order contribution to $P_{\delta\delta}^s$ is $P_{\theta_S\theta_S} u^4$ (Eq. 26), which enhances $P_{\delta\delta}^s$. Notice that, since \mathbf{v}_S is uncorrelated with the density field, it does not contribute a u^2 term as \mathbf{v}_δ does. Higher order contributions come from both fourth and higher order velocity correlations (Eq. 25) and from the convolution of ϵ_S with $\langle (1+\delta_1)(1+\delta_2) \exp \lambda_\delta \rangle$ (Eq. 15). These corrections are of the order δ^4 or higher. We group all these contributions into a single function $C_S(k, u)$ (Eq. 26). Later we argue that we may be able to set $C_S = 0$ in the RSD modeling.

On the other hand, \mathbf{v}_S causes an overall damping, characterized by D_S^{FOG} ,

$$\sqrt{D_S^{\text{FOG}}(ku)} = \int_{-\infty}^{\infty} \exp\left(i \frac{ku v_{z,S}}{H}\right) P_S(v_{z,S}) dv_{z,S}$$

$$= \int_{-\infty}^{\infty} \cos\left(\frac{ku v_{z,S}}{H}\right) P_S(v_{z,S}) dv_{z,S}.$$

Since \mathbf{v}_S arises from nonlinear evolution, it is intrinsically non-Gaussian. We will check if D^{FOG} can be well described by the first several cumulants, with the aid of the cumulant expansion theorem (Eq. 23).

C. The role of \mathbf{v}_δ

Due to coupling between the velocity and the density fields, redshift distortion induced by \mathbf{v}_δ is complicated, although analytical expression in the Gaussian limit exists [42]. We group the Gaussian terms with order higher than δ^2 as C_G . We also derive the non-Gaussian corrections and group them as C_{NG} in the appendix. Both terms are consequences of the \mathbf{v}_δ - δ correlation.

In Fourier space, we have

$$P_{\delta\delta}^s(k, u) = \left\{ P_{\delta\delta}(k)(1 + f\tilde{W}(k)u^2)^2 + u^4 P_{\theta_S\theta_S}(k) \right.$$

$$+ C_{NG}(k, u) + C_G(k, u) + C_S(k, u) \left. \right\}$$

$$\times D_\delta^{\text{FOG}}(ku) D_S^{\text{FOG}}(ku) D_B^{\text{FOG}}(ku). \quad (26)$$

Here, C_G and C_{NG} are the Fourier transforms of the corresponding terms in real space ($C_G(\mathbf{r}, k_z)$, Eq. A6 and $C_{NG}(\mathbf{r}, k_z)$, Eq. A8).

\mathbf{v}_δ also causes a FOG effect, described by D_δ^{FOG} . \mathbf{v}_δ is largely Gaussian due to the suppression of $\tilde{W} < 1$ in the nonlinear and non-Gaussian regime. However, due to the large amplitude of σ_{v_δ} , it is unclear whether we can neglect the K_4 and/or K_6 corrections. Here σ_{v_δ} is the one dimension velocity dispersion of \mathbf{v}_δ ,

$$\sigma_{v_\delta}^2 \equiv \langle v_{\delta,z}^2 \rangle = \frac{1}{3} \int \Delta_{v_\delta v_\delta}^2(k) \frac{dk}{k} \quad (27)$$

$$= \frac{1}{3} \int \frac{H^2}{k^2} \Delta_{\delta\delta}^2(k) W^2(k) \frac{dk}{k}.$$

The C_{NG} , C_G and C_S terms are the sums of infinite power series of δ . To carry out realistic calculation, we need to truncate them in a reasonable way. The first line terms in the right hand side of Eq. 26 exhaust contributions of the order δ^2 . It can be rewritten in a more familiar form $P_{\delta\delta} + 2u^2 P_{\delta\theta} + u^4 P_{\theta\theta}$ (e.g. [42]) and confirms previous results. The second line terms are higher order in δ . The leading order term of C_{NG} is $\propto \delta^3$, while those of C_G and C_S are $\propto \delta^4$. In this sense, for Eq. 26 to be complete at the order of δ^3 , we can set $C_G = 0$ and $C_S = 0$.

But in term of the linear density δ_L , the situation is different. (1) $P_{\theta_S\theta_S}$ vanishes in the linear perturbation theory, but emerges in the second or higher order Eulerian perturbation theory. So $P_{\theta_S\theta_S}$ itself is of the order δ_L^4 and C_S is of the order δ_L^6 . (2) In the Eulerian perturbation theory, leading order terms of C_G and C_{NG} are of the order δ_L^4 . So up to the order δ_L^4 , we can set $C_S = 0$.

Hence no matter in power series of δ or in power series of δ_L , we can set $C_S = 0$ when calculating the leading order corrections to the usual RSD formula. But whether or not we shall set $C_G = 0$ is an issue for numerical examination.

The inclusion of C_G and C_{NG} may appear to introduce more difficulties and uncertainties to the RSD modeling. However, this is not the case. We will show that, *the inclusion of C_G and leading order terms in C_{NG} does not introduce extra degrees of freedom in the RSD modeling*. So the inclusion of these terms is capable of reducing systematical errors, without degrading cosmological parameter constraints. This is definitely a desirable property, made possible by the proposed velocity decomposition.

1. The C_G correction

C_G is an analytical (but nonlinear) function of the two point density and velocity (\mathbf{v}_δ) correlation functions (Eq. A6). Since $P_{\delta\delta}$ is directly measurable from the $k_z = 0$ Fourier modes in redshift surveys, C_G up to any order can be calculated strictly without introduce any extra parameters.

C_G does not contain terms of odd order in δ . So we can split C_G as $C_G(k, u) = \sum_j C_{G,2j}(k, u)$ where $j = 2, 3 \dots$.

In reality, we may only need the leading order

$$C_{G,4}(k, u) = \int \frac{d^3 \mathbf{k}_1}{(2\pi)^3} P_{\delta\delta}(k_1) P_{\delta\delta}(k_2) \frac{k_{1z} k_{2z} k_z^2 W_1 W_2}{k_1^2 k_2^2} \times G(\mathbf{k}, \mathbf{k}_1, \mathbf{k}_2). \quad (28)$$

Here, $\mathbf{k}_2 = \mathbf{k} + \mathbf{k}_1$ and $W_i \equiv W(k_i)$. The kernel G is

$$G = \frac{k_{1z} W_1 / k_1^2}{k_{2z} W_2 / k_2^2} - 1 + \frac{2k_{1z} k_z W_1}{k_1^2} + \frac{k_{1z} k_{2z} k_z^2 W_1 W_2}{2k_1^2 k_2^2}. \quad (29)$$

With $P_{\delta\delta}$ an observable and W a function to be fitted anyway, calculating C_G requires no extra free parameters and hence does not induce new model uncertainties.

2. The C_{NG} correction

$C_{NG}(k, u) = \sum_{j \geq 3} C_{NG,j}(k, u)$ contains connected part of j -th order correlation ($\langle v_\delta^j \rangle$, $\langle \delta v_\delta^{j-1} \rangle$ and $\langle \delta \delta v_\delta^{j-2} \rangle$) to $j \rightarrow \infty$ (Eq. A8). These terms are the consequence of nonlinear and non-Gaussian evolution, so we expect them to become non-negligible only in nonlinear regime and may become dominant in deeply nonlinear regime. However, since $\tilde{W} \rightarrow 0$ in deeply nonlinear regime, their contributions to $P_{\delta\delta}^s$ are significantly suppressed. For the same reason, $C_{NG,j+1}$ is suppressed by a factor $\sim \tilde{W}$, with respect to $C_{NG,j}$. Hence we propose to keep only the $j = 3$ term and neglect higher order corrections.

Fourier transforming $C_{NG,3}(\mathbf{r}, k_z)$ (Eq. A8), we obtain

$$C_{NG,3}(k, u) = \int \frac{d^3 \mathbf{k}_1}{(2\pi)^3} B_3(\mathbf{k}_1, \mathbf{k}_2, \mathbf{k}) \frac{k_{1z} k_z}{k_1^2} W(k_1) \times \left[2 \frac{k_z^2}{k^2} W(k) + 2 \frac{k_z k_{2z}}{k_2^2} W(k_2) - 1 \right] \quad (30)$$

Here, $\mathbf{k}_2 = -\mathbf{k}_1 - \mathbf{k}$. $B_3(\mathbf{k}_1, \mathbf{k}_2, \mathbf{k}_3)$ is the real space matter bispectrum. We notice that the ensemble average of $B_3(\mathbf{k}_1, \mathbf{k}_2, \mathbf{k}_3)$ is directly available from the same redshift surveys used for RSD measurement. Since $\sum_i \mathbf{k}_i = 0$, \mathbf{k}_1 , \mathbf{k}_2 and \mathbf{k}_3 lie in the same plane. Due to the isotropy of the universe, $B_3(\mathbf{k}_1, \mathbf{k}_2, \mathbf{k}_3)$ does not depend on the inclination of the plane. So its value is equal to the case where all \mathbf{k} lie in the plane perpendicular to the line of sight (namely the x-y plane). Redshift distortion does not alter the $k_z = 0$ Fourier mode. Namely, $\delta^s(\mathbf{k}_\perp, k_z = 0) = \delta(\mathbf{k}_\perp, k_z = 0)$. This means that B_3 can be directly measured from the observed Fourier mode with $k_{i,z} = 0$. Hence including $C_{NG,3}$ in the calculation does not introduce extra fitting parameters and hence does not weaken the cosmological constraints.

The same trick does not apply to $C_{NG,j \geq 4}$. They involve 4-th or higher order correlation ($\delta(\mathbf{k}_1), \dots, \delta(\mathbf{k}_j)$), with $\mathbf{k}_1 + \dots + \mathbf{k}_j = 0$. In general, $\mathbf{k}_i (i = 1, 2, 3, 4 \dots, j)$ do not lie in the same plane. We are no longer able to infer their values from the $k_z = 0$ modes. However, due to extra suppression caused by $\tilde{W} < 1$, we do not expect these terms to be important. Nevertheless, the accuracy of neglecting these higher order terms must be quantified through N-body simulations.

D. A new formula on the redshift space power spectrum

We then propose the following formula for the redshift space power spectrum,

$$P^s(k, u) \simeq \left\{ P_{\delta\delta}(k) \left(1 + f \tilde{W}(k) u^2 \right)^2 + u^4 P_{\theta_S \theta_S}(k) + C_G(k, u) + C_{NG,3}(k, u) \right\} \times D_\delta^{\text{FOG}}(ku) D_S^{\text{FOG}}(ku) \exp \left[- \frac{k^2 u^2 \sigma_{v_B}^2}{H^2} \right]. \quad (31)$$

In Eq. 31, $W(k) \equiv f \tilde{W}(k)$ and $P_{\theta_S \theta_S}(k)$ are the cosmological information we seek for. We address one more time that, C_G and $C_{NG,3}$ are not free functions. They are uniquely determined by W . This valuable property is achieved by the proposed velocity decomposition and, in particular, by the deterministic relation $\theta_\delta = \delta W$.

There are only very limited degrees of freedom in the FOG terms. Through Eq. 23, $D_\delta^{\text{FOG}}(ku)$ and $D_S^{\text{FOG}}(ku)$ may be well described by σ_{v_δ} , σ_{v_S} and/or K_{4,v_δ} , K_{4,v_S} , K_{6,v_δ} , K_{6,v_S} . Among them, σ_{v_δ} is determined by W (Eq. 27) and σ_{v_S} is determined by $P_{\theta_S \theta_S}$. So in principle neither σ_{v_δ} nor σ_{v_S} are free parameters [86]. Furthermore, since $\sigma_{v_B}^2 \ll \sigma_{v_\delta}^2$ [1, 70], we may be able to set $\sigma_{v_B} = 0$, depending on the desired accuracy.

1. Comparing to existing models

Here we compare the proposed RSD formula (Eq. 31) with a few existing RSD formulae. We choose these formulae because they can be compared with ours relatively straightforwardly. So this comparison is by no means complete. For brevity, we focus on the matter power spectrum for which we do not need to worry about the galaxy bias, especially the nonlinear/non-deterministic bias. (1) The Kaiser formula plus the FOG effect (hereafter KF),

$$P_{\delta\delta}^s(k, u) \simeq P_{\delta\delta}(k) (1 + f u^2)^2 D^{\text{FOG}}(ku). \quad (32)$$

This is perhaps the most commonly used RSD formula. (2) The Desjacques & Sheth 2010 formula (hereafter DS10, [47]),

$$P_{\delta\delta}^s(k, u) = P_{\delta\delta}(k) (1 + f u^2)^2 \times \exp(-k_z^2 \sigma_v^2 / H^2) V_{\text{vir}}(k_z). \quad (33)$$

Here, V_{vir} is the damping caused by random motions of virialized particles in halos. σ_v is the velocity dispersion of bulk motion. It improves over the KF formula by correctly recognizing the two velocity components (bulk motion and random motion). (3) The Scoccimarro 2004 formula (hereafter S04, [42]),

$$P_{\delta\delta}^s(k, u) = (P_{\delta\delta}(k) + 2u^2 P_{\delta\theta}(k) + u^4 P_{\theta\theta}(k)) \times \exp(-k_z^2 \sigma_v^2 / H^2). \quad (34)$$

Here, σ_v can be treated as the one calculated from the perturbation theory or as a free parameter. It improves over KF by taking into account differences in the density and velocity nonlinear evolution. As a consequence, it does not assume a deterministic relation between density and velocity. (4) The Taruya et al. 2010 formula (hereafter T10, [53]),

$$P_{\delta\delta}^s(k, u) = (P_{\delta\delta}(k) + 2u^2 P_{\delta\theta}(k) + u^4 P_{\theta\theta}(k)) \quad (35) \\ + A(k, u) + B(k, u) \exp(-k^2 u^2 \sigma_v^2 / H^2).$$

The extra term A involves integral over the bispectrum. The term B involves convolution of two real space power spectra.

Comparing to Eq. 31, we recognize a number of corrections to existing formulae. Here we briefly summarize the most significant ones. (1) Both KF and DS10 fail to capture the \tilde{W} correction on f . So f based on KF and DS10 is underestimated by a factor \tilde{W} . (2) S04 and T10 improve over KF and DS10 by correctly capturing the \tilde{W} correction, although S04 and T10 do not make this correction explicitly. T10 further improves over S04 by including next order corrections (A and B). In the appendix B, we prove that $A = C_{NG,3}$ in the limit $\mathbf{v}_S \rightarrow 0$. However, T10 adopted the approximation $\epsilon_\delta = 0$ in some intermediate steps. so it fails to capture some terms of the same order as A and B , as we do (Eq. A7). More importantly, calculating A and B requires heavy modeling or simulation calibration. Our Eq. 31 avoids these uncertainties. (3) The FOG effect is caused by three distinctly different velocity components, so it may not follow a simple function form. For this point, the closest match to our formula is DS10. These complexities can bias the interpretation of the inferred σ_v from RSD.

E. Implications on the RSD cosmology

Our analysis above shows that what one can infer from RSD is the combination $f\tilde{W}(k)$ instead of f . Since $\tilde{W}(k) \sim 0.9$ at $k = 0.1h/\text{Mpc}$ and $z = 0$, this can cause 10% underestimation in f . We expect that it is at least a significant source causing the recently found underestimation in f [63–68]. This systematical error overwhelms the 1% level statistical accuracy in f by stage IV dark energy projects. With robust modeling of \tilde{W} , it is promising to eliminate this systematical error in the RSD cosmology.

The \tilde{W} correction affects many applications of redshift distortion. For example, [25] proposed an E_G estimator combining weak lensing and redshift distortion to test general relativity at cosmological scale. This estimator is insensitive to galaxy bias and is also less affected by initial fluctuations. [28] made the first E_G measurement and found $E_G = 0.39 \pm 0.06$ at an effective redshift 0.32 and $O(10)\text{Mpc}/h$ scale. This measurement confirms general relativity within $\sim 20\%$ observational uncertainties. This result has been used to perform consistency tests

of the ΛCDM cosmology and confirmed its validity [78]. Given the existence of $\tilde{W} \neq 1$, the expectation value of E_G should be corrected by a factor $1/\tilde{W}$,

$$E_G = \left[\frac{G_{\text{eff}} \Omega_0}{G_N f} \right] \frac{1}{\tilde{W}(k)}. \quad (36)$$

Future experiments such as BigBOSS+LSST, BigBOSS+Planck CMB lensing, Euclid, SKA or other combinations of spectroscopic surveys and imaging surveys are capable of measuring E_G to 1% level statistical accuracy [25]. For these measurements, The $1/\tilde{W}$ correction is needed in order to correctly interpret the measured E_G .

F. To do list

Most statistics discussed in this section are too complicated to evaluate analytically. In companion papers [1], we will use N-body simulations to numerically evaluate these statistics. An incomplete investigation list includes

- The damping function $D_\delta^{\text{FOG}}(ku)$, $D_S^{\text{FOG}}(ku)$ and $D_B^{\text{FOG}}(ku)$. In particular, we will investigate the usage of the cumulant expansion theorem (Eq. 23). We will check if including K_4 and/or K_6 describes $D_\delta^{\text{FOG}}(ku)$ and $D_S^{\text{FOG}}(ku)$ accurately at scales of interest. We will also check the accuracy of Eq. 24.
- ϵ_δ , ϵ_S and ϵ_B . In particular, we will quantify the accuracy of Eq. 21 & 25.
- The accuracy of the proposed RSD formula (Eq. 31). We will measure $C_{G,j}$ and $C_{NG,j}$ from simulations. We will also quantify the relative contribution of the leading terms, namely $C_{G,4}$ to C_G , $C_{NG,3}$ to C_{NG} and $P_{\theta_S\theta_S}$ with respect to C_S . We will seek the possibility to further improve the RSD modeling, if needed.

IV. RECONSTRUCTION OF THE 3D VELOCITY FIELD IN REDSHIFT SURVEYS

So far we focus on inferring the statistical average of the velocity field including $W \propto P_{\delta\theta}$, $P_{v_S v_S}$, σ_{v_δ} , σ_{v_S} and σ_{v_B} . Can we go a step further to construct the full 3D velocity field? The gain would be huge since the 3D velocity field contains much more information and has much more applications. One of such applications is the kinetic Sunyaev Zel'dovich (kSZ) tomography [79, 80].

The diffuse kinetic Sunyaev Zel'dovich (kSZ) effect [81] caused by the intergalactic medium is a potentially powerful probe for missing baryons. Unfortunately, measuring kSZ is very difficult, due to the weakness of the kSZ signal, the lack of spectral feature and various overwhelming contaminations such as primary CMB, the thermal SZ effect and cosmic infrared background. The

state of art experiments such as ACT [82, 83] and SPT [84, 85] has reported the first detection of the kSZ effect of galaxy clusters [83]. Nevertheless, the diffuse kSZ is still elusive.

The measurement can be revolutionized by the kinetic SZ tomography [79, 80]. The key is to reconstruct the galaxy velocity field and then construct the galaxy momentum field. We then correlate the projected momentum field with CMB to measure the kSZ effect. This kSZ tomography automatically eliminating all contaminations of scalar type. A combination of BigBOSS and Planck is promising to measure kSZ to better than 10σ at a number of redshift bins [80].

A. Proposals on the velocity reconstruction

How to reconstruct the 3D velocity field? If we can, which velocity component can be reconstructed? There are numerous works over a long history. We are not at a stage to overview these works. Rather, we outline our approach, based upon the proposed velocity decomposition.

Since observationally we only have the density field, which is a scalar field, the information budget does not allow us to reconstruct all the three \mathbf{v}_δ , \mathbf{v}_S and \mathbf{v}_B vector fields. However, since \mathbf{v}_δ is completely correlated with the density field, it is promising to reconstruct \mathbf{v}_δ from the observed density field. Eq. 3 guides us to propose a linear estimator for the 3D peculiar velocity reconstruction through the 3D density field. Since we observe the redshift space overdensity δ^s instead, this linear estimator should operate on $\delta^s(\mathbf{k})$,

$$\hat{\theta}_\delta(\mathbf{k}) = \delta^s(\mathbf{k})\hat{W}^s(\mathbf{k}) . \quad (37)$$

We use the superscript “s” to denote properties in redshift space. \hat{W}^s corresponds to an anisotropic window function operating on the anisotropic density field in redshift space. Now the reconstruction of the stochastic 3D velocity field is simplified into the reconstruction of a deterministic function W^s . Due to the axial symmetry along the light of sight, $W^s(\mathbf{k}) = W^s(k, u)$. So it only has 2D degrees of freedom. These degrees of freedom are further limited by the asymptotic behaviors of $W^s(k, u)$ at $ku \rightarrow 0$ and at $k \rightarrow \infty$.

We want the peculiar velocity estimator (Eq. 37) to have no multiplicative error. This requires

$$\hat{W}^s(\mathbf{k}) = \frac{W(k)}{C_v(\mathbf{k})} = \frac{W(k)}{r_{\delta\delta^s}(\mathbf{k})} \sqrt{\frac{P_{\delta\delta}(k)}{P_{\delta\delta^s}^s(\mathbf{k})}} . \quad (38)$$

W^s differs from the real space one by a direction dependent factor $1/C_v(\mathbf{k})$. This factor arises because the redshift space density δ^s is not completely correlated with the real space density δ . To better understand this point and to derive Eq. 38, we carry out a decomposition of δ^s into two parts,

$$\delta^s = \delta_v^s + \delta_S^s . \quad (39)$$

We require δ_v^s to be completely correlated with the underlying overdensity δ and hence to θ_δ . This is the part that we can use to recover the peculiar velocity. For this reason, we label this part with a subscript “v”. δ_S^s is uncorrelated with δ and θ_δ . It causes the stochasticity in δ - δ^s relation and contaminates the velocity reconstruction. So it is labelled with a subscript “S”. Since δ_v is completely correlated with δ ,

$$\delta_v^s(\mathbf{k}) = \delta(\mathbf{k})C_v(\mathbf{k}) , \quad (40)$$

with the deterministic function C_v to be determined. Through the relation $\langle \delta(\mathbf{k})\delta^s(\mathbf{k}') \rangle = \langle \delta(\mathbf{k})\delta_v^s(\mathbf{k}') \rangle = \langle \delta(\mathbf{k})\delta(\mathbf{k}') \rangle C_v(\mathbf{k})$, we obtain

$$C_v(\mathbf{k}) = \frac{P_{\delta\delta^s}(\mathbf{k})}{P_{\delta\delta}(k)} = r_{\delta\delta^s}(\mathbf{k}) \sqrt{\frac{P_{\delta\delta}^s(k, u)}{P_{\delta\delta}(k)}} . \quad (41)$$

Here, $P_{\delta\delta^s}$ is the cross power spectrum between δ and δ^s . $r_{\delta\delta^s}$ is the corresponding cross correlation coefficient. It has the asymptotic behavior $r_{\delta\delta^s} \rightarrow 1$ when $ku \rightarrow 0$ and $r_{\delta\delta^s} \rightarrow 0$ when $ku \rightarrow \infty$. Notice that $r_{\delta\delta^s}$ depends on both k and u . So do C_v and W^s . Hereafter we will write them as $r_{\delta\delta^s}(k, u)$, $W^s(k, u)$ and $C_v(k, u)$ to highlight these dependences.

Both $P_{\delta\delta}(k)$ and $P_{\delta\delta^s}^s(k, u)$ are observables. To evaluate \hat{W}^s requires just one extra input, $r_{\delta\delta^s}(k, u)$. $r_{\delta\delta^s}$ has a well defined asymptotic behavior $r_{\delta\delta^s} \rightarrow 1$ when $ku \rightarrow 0$ and $r_{\delta\delta^s} \rightarrow 0$ when $|ku| \rightarrow \infty$. In the appendix C, we show that r is uniquely fixed by W and other quantities which can be inferred from $P_{\delta\delta}^s(k, u)$. Hence the observed RSD allows us to figure out W^s and then carry out the velocity reconstruction. In this sense, *RSD is a source of information crucial for the velocity reconstruction, instead of source of noise as in many other approaches of velocity reconstruction.*

In the appendix D, we propose another approach to reconstruct the 3D velocity field. It shows more clearly the crucial role of RSD in the velocity reconstruction.

B. Reconstruction errors and remedies

A correct $W^s(k, u)$ allows to reconstruct \mathbf{v}_δ free of multiplicative error. Unfortunately, additive errors persist, due to the stochastic component δ_S^s . The reconstructed velocity divergence is

$$\begin{aligned} \hat{\theta}_\delta(\mathbf{k}) &= \theta_\delta(\mathbf{k}) + \theta_S^s(\mathbf{k}) , \\ \theta_S^s(\mathbf{k}) &\equiv \delta_S^s(\mathbf{k})\hat{W}^s(k, u) . \end{aligned} \quad (42)$$

The additive error in the reconstructed velocity is then

$$v_S^s(\mathbf{k}) = \frac{iH\theta_S^s(\mathbf{k})\mathbf{k}}{k^2} . \quad (43)$$

If we measure the velocity power spectrum directly through the reconstructed velocity field, it will suffer

from an additive error. So cosmological applications of the directly measured auto power spectrum can be very limited, if any. Fortunately, one can circumvent this problem straightforwardly.

We start with a valuable property, that the cross power spectrum between the reconstructed velocity and the density distribution is unbiased,

$$\hat{P}_{\delta\theta} = P_{\delta\theta} = P_{\delta\theta\delta} . \quad (44)$$

For the same reason, the additive error does not bias the kSZ tomography [79, 80] and hence does not bias the effort to search for missing baryons.

Since θ_δ is completely correlated with the matter density, we can measure the auto power spectrum, through the relation

$$P_{\theta_\delta\theta_\delta} = \frac{P_{\delta\theta\delta}^2}{P_{\delta\delta}} . \quad (45)$$

The auto power spectrum measured in this way is free of additive error discussed above.

C. To do list

Through N-body simulations, a number of key issues will be investigated in future works,

- $r_{\delta\delta^s}(k, u)$, $W^s(k, u)$ and $C_v(k, u)$. We are then able to quantify the additive error in the reconstructed velocity. Furthermore, we want to understand the origin of δ_g^s , which causes the stochasticity in the δ - δ^s relation and degrades the reconstruction performance.
- The accuracy of Eq. C6 to model $r_{\delta\delta^s}$.
- The accuracy of the velocity reconstruction. It is determined by the accuracy of the inferred W from the observed RSD and the accuracy of the modeled $r_{\delta\delta^s}$. Measurement errors in the galaxy distribution such as shot noise further complicates the reconstruction. We will take them into account for more realistic quantification of the reconstruction performance.
- Further investigation of the velocity reconstruction approach proposed in the appendix D.

V. FROM MATTER DISTRIBUTION TO GALAXY DISTRIBUTION

In reality, we have 3D galaxy distribution instead of 3D matter distribution. The matter-galaxy relation is complicated. Nevertheless, the above methods to model the matter redshift space distortion and to carry out velocity reconstruction can be extended to the 3D galaxy distribution straightforwardly and robustly. The procedure is as follows.

A. The redshift space galaxy power spectrum

First, we decompose the galaxy velocity \mathbf{v}_g into an irrotational part $\mathbf{v}_{E,g}$ and a rotational part $\mathbf{v}_{B,g}$. For clarity, we use the subscript ‘‘g’’ to denote galaxy properties. This step is essentially the same as the case of the matter field.

But the next step is different. Now we need to decompose the irrotational galaxy velocity $\mathbf{v}_{E,g}$ into two eigenmodes such that one part (\mathbf{v}_{δ_g}) is completely correlated with the galaxy overdensity δ_g and the other part ($\mathbf{v}_{S,g}$) is completely uncorrelated with δ_g . Following §II, we obtain the θ_{δ_g} - δ_g relation,

$$\theta_{\delta_g}(\mathbf{k}) = W_g(k)\delta_g(\mathbf{k}) . \quad (46)$$

Here θ_{δ_g} is the divergence of \mathbf{v}_{δ_g} . The window function W_g is given by

$$W_g(k) \equiv \frac{P_{\delta_g\theta_g}(k)}{P_{\delta_g\delta_g}(k)} . \quad (47)$$

We recognize that $W_g(k \rightarrow 0) = f/b_g(k \rightarrow 0) = \beta$. Here, $b_g(k \rightarrow 0)$ is the linear galaxy bias. We have assumed no galaxy velocity bias at sufficiently large scale. We also define

$$\tilde{W}_g(k) \equiv \frac{W_g(k)}{W_g(k \rightarrow 0)} = \frac{W_g(k)}{\beta} = \frac{1}{\beta} \frac{P_{\delta_g\theta_g}}{P_{\delta_g\delta_g}} . \quad (48)$$

One can compare Eq. 46, 47, 48 with Eq. 3, 4, 5, respectively. There are important differences. For example, W and W_g differ by a factor b_g at large scale. Consequently, the relation $W = f\tilde{W}$ is replaced by $W_g = \beta\tilde{W}_g$.

The final step is to replace quantities of the matter field in previous sections by corresponding galaxy quantities to obtain results applicable to the galaxy field. The transformation is,

$$\begin{aligned} \delta \rightarrow \delta_g , \quad \theta \rightarrow \theta_g , \quad W \rightarrow W_g , \quad \tilde{W} \rightarrow \tilde{W}_g , \quad f \rightarrow \beta , \quad (49) \\ \mathbf{v} \rightarrow \mathbf{v}_g , \quad \mathbf{v}_\delta \rightarrow \mathbf{v}_{\delta_g} , \quad \mathbf{v}_S \rightarrow \mathbf{v}_{S,g} , \quad \mathbf{v}_B \rightarrow \mathbf{v}_{B,g} , \\ D_\delta \rightarrow D_{\delta_g} , \quad D_S \rightarrow D_{S,g} , \quad D_B \rightarrow D_{B,g} , \quad \dots \end{aligned}$$

We explicitly show one example. In §IIID, we suggest to use Eq. 31 to model the matter power spectrum in redshift space. Applying the above transformation (Eq. 49) to Eq. 31, we obtain the formula for the redshift space galaxy power spectrum,

$$\begin{aligned} P_{\delta_g\delta_g}^s(k, u) \simeq & \left\{ P_{\delta_g\delta_g}(k)(1 + \beta\tilde{W}_g(k)u^2)^2 \right. \\ & + u^4 P_{\theta_{S,g}\theta_{S,g}}(k) + C_{G,g}(k, u) + C_{NG,3g}(k, u) \left. \right\} \\ & \times D_{\delta_g}^{\text{FOG}}(ku) D_{S,g}^{\text{FOG}}(ku) \exp \left[-\frac{k^2 u^2 \sigma_{v_{B,g}}^2}{H^2} \right] . \end{aligned} \quad (50)$$

Here, $C_{NG,3g}$ and $C_{G,g}$ are defined by applying the transformation in Eq. 49 to Eq. A8 and A6. In the limit $k \rightarrow 0$, we recover the correct behavior $P_{\delta_g\delta_g}^s \rightarrow P_{\delta_g\delta_g}(1 + \beta u^2)^2$.

B. On the interpretation of E_G

The above transformation is in general straightforward to apply. Nevertheless, extra care should be given for some special cases. For example, it turns out that the \tilde{W} in the E_G estimator (Eq. 36) may still be interpreted as that of the matter field instead of the galaxy field, for the complexity that it involves not only the galaxy field (redshift distortion), but also the matter field (weak lensing) and the galaxy field.

By construction, E_G is proportional to the ratio of galaxy-lensing cross correlation and galaxy-velocity cross correlation [25]. Namely $E_G \propto P_{\delta_g \delta} / P_{\delta_g \theta_g}$. Notice that δ is the matter overdensity. In the large scale limit $\mathbf{v}_{\delta_g} \rightarrow \mathbf{v}_\delta$ ($\theta_{\delta_g} \rightarrow \theta_\delta = \delta W$), we have $E_G \propto 1/W = 1/(f\tilde{W})$, even for the galaxy field. This property is desirable since the correction term \tilde{W} can be robustly quantified through N-body simulations, free of uncertainties in modeling galaxy formation. Nevertheless, we shall use simulations to quantify the accuracy of the key approximation $\theta_{\delta_g} \simeq \theta_\delta$ and the scale where this approximation breaks.

C. Velocity reconstruction through 3D galaxy distribution

Following the case of velocity reconstruction through 3D redshift space matter distribution, we derive the linear estimator to reconstruct \mathbf{v}_{δ_g} from 3D redshift space galaxy overdensity δ_g^s ,

$$\hat{\theta}_{\delta_g}(\mathbf{k}) = \delta_g^s(\mathbf{k}) \hat{W}_g^s(\mathbf{k}). \quad (51)$$

The anisotropic window function $\hat{W}_g^s(\mathbf{k})$ is derived to be

$$\hat{W}_g^s(\mathbf{k}) = \frac{W_g(k)}{C_{v,g}(\mathbf{k})} = \frac{W_g(k)}{r_{\delta_g \delta_g^s}(\mathbf{k})} \sqrt{\frac{P_{\delta_g \delta_g}(k)}{P_{\delta_g \delta_g^s}^s(\mathbf{k})}}. \quad (52)$$

Here, $r_{\delta_g \delta_g^s}$ is the cross correlation coefficient between the real space δ_g and the redshift space δ_g^s . It can be computed by applying the transformation Eq. 49 to Eq. C6. One can compare between Eq. 37 & 51 and between Eq. 38 & 52 for similarities and differences.

Our velocity reconstruction method significantly alleviates the problem of galaxy bias in some existing velocity reconstruction methods. Even better, in the limit of a deterministic bias ($\delta_g = b_g \delta$), it completely overcomes it. Since $\hat{W}_g \propto 1/b_g$, the reconstructed 3D velocity is $\propto W_g \delta_g \propto b_g^0$, independent of b_g . This is also the case for the inferred velocity power spectrum,

$$P_{\theta_{\delta_g} \theta_{\delta_g}}(k) = \frac{P_{\delta_g \theta_{\delta_g}}^2(k)}{P_{\delta_g \delta_g}(k)} \propto b_g^0. \quad (53)$$

In future works we will redo the numerical analysis of the matter density field for the halo number density field,

through N-body simulations of $O(10)$ Gpc³ volume in total. We will then proceed to mock catalogs of galaxies. Eventually we plan to develop efficient and sophisticated codes applicable to real data of spectroscopic redshift surveys.

VI. DISCUSSIONS AND SUMMARY

We have laid out the methodology to carry out 3D velocity reconstruction from 3D matter and galaxy distribution. The method is based upon a velocity decomposition into three eigen-modes with physical motivation and of mathematical uniqueness. The same decomposition also helps us to derive a potentially more robust RSD formula. Through it we find that the inferred structure growth rate based upon some simplified versions of RSD modeling can be severely underestimated. In a series of companion papers [1] we will analyze N-body simulations to measure statistics of the three velocity eigen-modes, to test the accuracy of the proposed RSD formula and to quantify the performance of the proposed velocity reconstruction.

Acknowledgments

This work was supported by the national science foundation of China (grant No. 11025316 & 11121062 and 10873035 & 11133003), National Basic Research Program of China (973 Program) under grant No.2009CB24901 and the CAS/SAFEA International Partnership Program for Creative Research Teams (KJJCX2-YW-T23).

Appendix A: Calculating the \mathbf{v}_δ induced RSD

Throughout this section we only deal with the velocity component \mathbf{v}_δ . Hence for brevity we neglect the subscript “ δ ” and denote $v_{1z,\delta} = v_1$, $v_{2z,\delta} = v_2$, $\lambda_{1,2} \equiv ik_z v_{1,2}/H$ and $\lambda_\delta \equiv \lambda_1 - \lambda_2$. We will adopt two tricks in [42, 53] to facilitate the derivation. The first is the relation $\langle \delta_1 \exp \lambda_\delta \rangle = \frac{\partial}{\partial a_1} \langle \exp(\lambda_\delta + a_1 \delta_1) \rangle_{a_1=0}$. In combination with the cumulant expansion theorem $\langle \exp X \rangle = \exp(\sum \langle X^n \rangle_c / n!)$, we have

$$\begin{aligned} \langle \delta_1 \exp \lambda_\delta \rangle &= \langle \exp \lambda_\delta \rangle \sum_{n \geq 1} \frac{n \langle \lambda_\delta^{n-1} \delta_1 \rangle_c}{n!} \\ &= \langle \exp \lambda_\delta \rangle \sum_{n \geq 0} \frac{\langle \lambda_\delta^n \delta_1 \rangle_c}{n!} \\ &= \langle \exp \lambda_\delta \rangle \sum_{n \geq 0} \frac{\langle \lambda_\delta^n \delta_1 \rangle_c}{n!}. \end{aligned} \quad (A1)$$

The second relation is $\langle \delta_1 \delta_2 \exp \lambda_\delta \rangle = \frac{\partial^2}{\partial a_1 \partial a_2} \langle \exp(\lambda_\delta + a_1 \delta_1 + a_2 \delta_2) \rangle_{a_1=0, a_2=0}$. Again with the cumulant expansion

sion theorem, we have

$$\langle \delta_1 \delta_2 \exp \lambda_\delta \rangle = \langle \exp \lambda_\delta \rangle \times \quad (\text{A2})$$

$$\left[\sum_{j \geq 1} \frac{\langle \lambda_\delta^j \delta_1 \rangle_c}{j!} \sum_{n \geq 1} \frac{\langle \lambda^n \delta_2 \rangle_c}{n!} + \sum_{n \geq 0} \frac{\langle \delta_1 \delta_2 \lambda_\delta^n \rangle_c}{n!} \right].$$

Putting all pieces together, we obtain

$$\langle (1 + \delta_1)(1 + \delta_2) \exp \lambda_\delta \rangle = D_\delta^{\text{FOG}}(k_z)(1 + \epsilon_\delta(\mathbf{r}, k_z))$$

$$\left(1 + \sum_{n \geq 1} \frac{\langle \lambda_\delta^n (\delta_1 + \delta_2) \rangle_c}{n!} + \sum_{n \geq 0} \frac{\langle \delta_1 \delta_2 \lambda_\delta^n \rangle_c}{n!} \right. (\text{A3})$$

$$\left. + \sum_{j \geq 1} \frac{\langle \lambda_\delta^j \delta_1 \rangle_c}{j!} \sum_{n \geq 1} \frac{\langle \lambda_\delta^n \delta_2 \rangle_c}{n!} \right).$$

Through the cumulant expansion theorem, we have

$$1 + \epsilon_\delta(\mathbf{r}, k_z) = \exp \left[\sum_{\alpha + \beta \geq 2} \frac{\langle \lambda_\delta^{\alpha + \beta} \rangle_c}{(\alpha + \beta)!} - \frac{\langle \lambda_\delta^\alpha \rangle_c \langle -\lambda_\delta^\beta \rangle_c}{\alpha! \beta!} \right]$$

$$= \exp \left[\frac{k_z^2 \langle v_1 v_2 \rangle}{H^2} + O(v^4) \right]. \quad (\text{A4})$$

Here, terms odd in the power of v vanish. For example, due to symmetry of $v \leftrightarrow -v$, we have $\langle (v_1 - v_2)^3 \rangle = 0$, $\langle v_1^3 \rangle = \langle v_2^3 \rangle$, and hence $\langle v_1 v_2^2 \rangle - \langle v_1^2 v_2 \rangle = 0$. For this reason, the next leading order terms in Eq. A4 is of the order v^4 , whose exact expression can be obtained following Eq. 25.

Collecting terms of the same orders together, we have

$$\langle (1 + \delta_1)(1 + \delta_2) \exp \lambda_\delta \rangle = D_\delta^{\text{FOG}}(k_z)$$

$$\times \left[1 + \langle \delta_1 \delta_2 \rangle + i \frac{k_z}{H} \langle \delta_2 v_1 - \delta_1 v_2 \rangle + \frac{k_z^2}{H^2} \langle v_1 v_2 \rangle \right. (\text{A5})$$

$$\left. + C_{NG}(\mathbf{r}, k_z) + C_G(\mathbf{r}, k_z) \right].$$

Two correction terms C_G and C_{NG} show up. Both arise from the nonlinear real space-redshift space mapping. But C_G exhausts all high order corrections if the density and velocity fields are Gaussian. So we denote it with a subscript ‘‘G’’. It has an exact analytical expression,

$$C_G(\mathbf{r}, k_z) = \left[\exp \left(\frac{k_z^2 \langle v_1 v_2 \rangle}{H^2} \right) - 1 \right]$$

$$\times \left(\langle \delta_1 \delta_2 \rangle + i \frac{k_z}{H} \langle \delta_2 v_1 - \delta_1 v_2 \rangle \right) \quad (\text{A6})$$

$$+ \frac{k_z^2}{H^2} \langle \delta_1 v_2 \rangle \langle \delta_2 v_1 \rangle \exp \left(\frac{k_z^2 \langle v_1 v_2 \rangle}{H^2} \right)$$

$$+ \left[\exp \left(\frac{k_z^2 \langle v_1 v_2 \rangle}{H^2} \right) - \frac{k_z^2}{H^2} \langle v_1 v_2 \rangle - 1 \right].$$

We notice that this analytical result for Gaussian field has been derived by [42] and shown as their Eq. 32.

As shown in §III, C_G can be robustly calculated combining observations without knowing the underlying cosmology and without introducing extra unknown parameters. The leading order term is 4-th power in the density field, with

$$C_{G,4}(\mathbf{r}, k_z) = \frac{k_z^2 \langle v_1 v_2 \rangle}{H^2} \left(\langle \delta_1 \delta_2 \rangle + i \frac{k_z}{H} \langle (v_1 - v_2)(\delta_1 + \delta_2) \rangle \right)$$

$$+ \frac{k_z^2}{H^2} \langle \delta_1 v_2 \rangle \langle \delta_2 v_1 \rangle + \frac{1}{2} \frac{k_z^4}{H^4} \langle v_1 v_2 \rangle^2. \quad (\text{A7})$$

C_{NG} exhausts all high order corrections arising from non-Gaussianities in the density and velocity fields. For this reason, we denote it with the subscript ‘‘NG’’. It is the sum of an infinite series of j -th order correlations with $j \geq 3$.

$$C_{NG} = \sum_{j \geq 3} C_{NG,j}(\mathbf{r}, k_z) \quad (\text{A8})$$

$$= \left[i \frac{k_z \langle \delta_1 \delta_2 (v_1 - v_2) \rangle_c}{H} - \frac{k_z^2 \langle (v_1 - v_2)^2 (\delta_1 + \delta_2) \rangle_c}{2H^2} \right]$$

$$+ \dots$$

In the above equation, we only show the explicit expression of $C_{NG,j=3}$.

So far the results are exact. However, to realistically evaluate C_{NG} , we need to truncate somewhere in the $C_{NG,j}$ series. We argue that, due to extra suppression $\tilde{W} \ll 1$ in the deeply nonlinear region, $j > 3$ terms should be smaller than $C_{NG,j=3}$. So it may be reasonably accurate to keep only $C_{NG,j=3}$. Nevertheless, we will check this approximation through N-body simulations and investigate if $C_{NG,j \geq 4}$ should be included in the calculation.

In the appendix B, we will prove that $C_{NG,j=3}$ is equivalent to the term A in [53]. Strictly speaking, its Fourier transform $C_{NG,j=3}(k, u) = A(k, u)$ in the limit of $\mathbf{v}_S \rightarrow 0$.

Appendix B: The $C_{NG,3-A}$ relation

The term A is derived by [53] as an additive correction to the Kaiser formula. [53] does not distinguish between \mathbf{v}_δ and \mathbf{v}_S , so the velocity showing up in the expression of A is $\mathbf{v}_E = \mathbf{v}_\delta + \mathbf{v}_S$. We consider the limit $\mathbf{v}_S = 0$. Re-expressed in our notations, A in [53] is

$$A(k, u) = i \frac{k_z}{H} \int \langle (v_1 - v_2) (\delta_1 - \frac{\nabla_1 v_1}{H}) (\delta_2 - \frac{\nabla_2 v_2}{H}) \rangle$$

$$\exp(-i \mathbf{k} \cdot \mathbf{r}) d^3 \mathbf{r} \quad (\text{B1})$$

$$= i k_z \int \langle (v_1 - v_2) \delta_1 \delta_2 \rangle \exp(-i \mathbf{k} \cdot (\mathbf{r}) d^3 \mathbf{r}$$

$$+ i \frac{k_z}{H^2} \int \langle (v_2 \delta_2 \nabla_1 v_1 - v_1 \delta_1 \nabla_2 v_2 + \delta_1 v_2 \nabla_2 v_2$$

$$- \delta_2 v_1 \nabla_1 v_1) \rangle \exp(i \mathbf{k} \cdot (\mathbf{x}_1 - \mathbf{x}_2)) d^3 \mathbf{x}_1 d^3 \mathbf{x}_2 \frac{1}{V}$$

$$+ i \frac{k_z}{H^3} \langle (v_1 - v_2) \nabla_1 v_1 \nabla_2 v_2 \rangle \exp(i\mathbf{k} \cdot (\mathbf{x}_1 - \mathbf{x}_2)) d^3 \mathbf{x}_1 d^3 \mathbf{x}_2 \frac{1}{V}.$$

Here V is the total volume. Since $v_2 \delta_2 \nabla_1 v_1 \exp(i\mathbf{k} \cdot \mathbf{x}_1) = \nabla_1 [v_2 \delta_2 v_1 \exp(i\mathbf{k} \cdot \mathbf{x}_1)] - ik_z v_2 \delta_2 v_1 \exp(i\mathbf{k} \cdot \mathbf{x}_1)$ and since $\nabla_1(\dots)$ integrates to zero, the term $v_2 \delta_2 \nabla_1 v_1$ in the above equation can be replaced by the term $-ik_z v_2 \delta_2 v_1$. In total we can do the following replacements in Eq. B1,

$$\begin{aligned} v_2 \delta_2 \nabla_1 v_1 &\rightarrow -ik_z v_2 \delta_2 v_1, \\ v_1 \delta_1 \nabla_2 v_2 &\rightarrow ik_z v_1 \delta_1 v_2, \\ \delta_1 v_2 \nabla_2 v_2 &\rightarrow ik_z \frac{1}{2} \delta_1 v_2^2, \\ \delta_2 v_1 \nabla_1 v_1 &\rightarrow -ik_z \frac{1}{2} \delta_2 v_1^2, \\ v_1 \nabla_1 v_1 \nabla_2 v_2 &\rightarrow k_z^2 \frac{1}{2} v_1^2 v_2, \\ v_2 \nabla_1 v_1 \nabla_2 v_2 &\rightarrow k_z^2 \frac{1}{2} v_2^2 v_1 \end{aligned} \quad (\text{B2})$$

Comparing to Eq. A7, we prove that, in the limit $\mathbf{v}_S \rightarrow 0$, $C_{NG,3}(k, u) = A(k, u)$.

On the other hand, our $C_{G,4}$ is not equal to the B term in [53], due to differences in the methods and differences in approximations made. For example, [53] sets $\epsilon_\delta = 0$ in their Eq. 18. Inclusion of $\epsilon_\delta \neq 0$ in our derivation brings up new terms such as the term $\langle v_1 v_2 \rangle^2$ in Eq. A8. In future works we will test against N-body simulations to compare the two results.

Appendix C: Modeling $r_{\delta\delta^s}(k, u)$

Following the derivation of $P_{\delta\delta^s}^s$, the real space -redshift space density cross power spectrum $P_{\delta\delta^s}$ is given by

$$\begin{aligned} P_{\delta\delta^s}(k, u) &= \int \langle (1 + \delta_1)(1 + \delta_2) \exp[ik_z v_{1z}/H] \rangle \exp(-i\mathbf{k} \cdot \mathbf{r}) d^3 \mathbf{r} \\ &= \int \left\langle (1 + \delta_1)(1 + \delta_2) \exp\left(i \frac{k_z v_{1\delta,z}}{H}\right) \right\rangle \exp(-i\mathbf{k} \cdot \mathbf{r}) d^3 \mathbf{r} \sqrt{D_S^{\text{FOG}}(k_z) D_B^{\text{FOG}}(k_z)}. \end{aligned} \quad (\text{C1})$$

Replacing λ_δ in Eq. A3 with λ_1 , we obtain

$$\begin{aligned} \langle (1 + \delta_1)(1 + \delta_2) \exp \lambda_1 \rangle &= \langle \exp \lambda_1 \rangle \\ \left(1 + \sum_{n \geq 1} \frac{\langle \lambda_1^n (\delta_1 + \delta_2) \rangle_c}{n!} + \sum_{n \geq 0} \frac{\langle \delta_1 \delta_2 \lambda_1^n \rangle_c}{n!} \right. \\ &\quad \left. + \sum_{j \geq 1} \frac{\langle \lambda_1^j \delta_1 \rangle_c}{j!} \sum_{n \geq 1} \frac{\langle \lambda_1^n \delta_2 \rangle_c}{n!} \right). \end{aligned} \quad (\text{C2})$$

We then have

$$\begin{aligned} P_{\delta\delta^s}(k, u) &= \left[P_{\delta\delta}(k)(1 + f\tilde{W}(k)u^2) + C_{NG}^{rs}(k, u) \right] \sqrt{D_\delta^{\text{FOG}}(k_z) D_S^{\text{FOG}}(k_z) D_B^{\text{FOG}}(ku)}. \end{aligned} \quad (\text{C3})$$

The high order correction term

$$\begin{aligned} C_{NG}^{rs}(k, u) &= y \times P_{\delta\delta}(k) f\tilde{W}u^2 + \int \exp(-i\mathbf{k} \cdot \mathbf{r}) d^3 \mathbf{r} \\ &\quad \times \left[\sum_{n \geq 1} \frac{\langle \delta_1 \delta_2 \lambda_1^n \rangle_c}{n!} + \sum_{n \geq 2} \frac{\langle \lambda_1^n \delta_2 \rangle_c}{n!} (1 + y) \right]. \end{aligned} \quad (\text{C4})$$

Here, $y \equiv \sum_{j \geq 1} \langle \lambda_1^j \delta_1 \rangle_c / j! = \sum_{j \geq 2} \langle \lambda_1^j \delta_1 \rangle_c / j!$. We can resum C_{NG}^{rs} in order of the power of δ ,

$$\begin{aligned} C_{NG}^{rs}(k, u) &= \sum_{j \geq 3} C_{NG,j}^{rs}(k, u) \\ &= \int e^{-i\mathbf{k} \cdot \mathbf{r}} d^3 \mathbf{r} \left[\langle \delta_1 \delta_2 \lambda_1 \rangle_c + \frac{\langle \lambda_1^2 \delta_2 \rangle_c}{2!} \right] + \dots \end{aligned} \quad (\text{C5})$$

The last expression only shows $C_{NG,3}^{rs}$. Finally we obtain the expression for $r_{\delta\delta^s}$,

$$r_{\delta\delta^s}(k, u) \simeq \frac{1 + \frac{C_{NG,3}^{rs}(k, u)}{P_{\delta\delta}(k)(1+f\tilde{W}(k)u^2)}}{\sqrt{1 + \frac{P_{\theta_S \theta_S}(k)u^4 + C_{NG,3}(k, u) + C_G(k, u)}{P_{\delta\delta}(k)(1+f\tilde{W}(k)u^2)}}}}. \quad (\text{C6})$$

Evaluating $r_{\delta\delta^s}$ requires $P_{\delta\delta}$, B_3 , W and $P_{\theta_S \theta_S}$. The first two quantities are observables, as discussed in §III. The last two can be inferred from the observed $P_{\delta\delta}^s$ (§IIID). So there is little uncertainty involved in predicting $r_{\delta\delta^s}$. This will also be the case for the window function W^s (Eq. 38) required for velocity reconstruction.

Appendix D: An alternative approach to reconstruct the 3D velocity field

As shown in §IV, the key to reconstruct the 3D \mathbf{v}_δ is to infer the correct window function W^s . The approach discussed in §IV is straightforward. But it relies on the RSD modeling and is hence susceptible to inaccuracies therein. Here we propose an alternative to simultaneously estimate W^s and reconstruct \mathbf{v}_δ . It avoids modeling the \mathbf{v}_δ induced RSD, the most difficult part in the RSD modeling. So it is less susceptible to uncertainties in the RSD modeling.

The guideline is that, if we construct W^s and \mathbf{v}_δ correctly, we can move particles/galaxies back to their real space positions. This will eliminate the \mathbf{v}_δ induced RSD and hence reduce anisotropies in the power spectrum after moving (hereafter we denote it as $P_{\text{move}}^s(\mathbf{k})$). To further demonstrate this point, let us consider the limit of $\mathbf{v}_S = 0$, $\mathbf{v}_B = 0$, $\delta_S^s = 0$ and no measurement noise. Under this limit, a correct guess of W^s will faithfully recover \mathbf{v}_δ . Moving the particles back to their real space positions using this \mathbf{v}_δ , anisotropies in $P_{\text{move}}(\mathbf{k})$ will be completely eliminated and we recover the isotropic real space power spectrum ($P_{\text{move}}(\mathbf{k}) = P(k)$). This suggests that, by tuning W^s until the $P_{\text{move}}(\mathbf{k})$ reaches isotropy, we can recover the correct W^s and hence reconstruct the velocity correctly.

The real situation is more complicated, due to the fact that $\mathbf{v}_S \neq 0$, $\mathbf{v}_B \neq 0$, $\delta_S^s \neq 0$ and the existence of measurement noise such as shot noise in the galaxy number distribution. However, none of them is correlated with the real space density and none of them can cause anisotropic pattern the same as \mathbf{v}_δ . This significantly simplifies the modeling of P_{move} . After we move the particles back according to \mathbf{v}_δ reconstructed with the correct W^s (no multiplicative error), we have

$$P_{\text{move}}(k, u) = \int (1 + \langle \delta_1 \delta_2 \rangle) D_{\text{move}}(k_z, \mathbf{r}) e^{-i\mathbf{k} \cdot \mathbf{r}} d^3\mathbf{r} \quad (\text{D1})$$

Like P^s , P_{move} only depends on k and u . So we write these dependences explicitly. Here

$$D_{\text{move}}(k_z, \mathbf{r}) \equiv \left\langle e^{\lambda_S + \lambda_B - ik_z(v_{1z,S}^s - v_{2z,S}^s)/H} \right\rangle. \quad (\text{D2})$$

v_S^s is the additive error defined in Eq. 43. We also define a ϵ_{move} through

$$1 + \epsilon_{\text{move}}(k_z, \mathbf{r}) \equiv \frac{D_{\text{move}}(k_z, \mathbf{r})}{D_{\text{move}}(k_z, r \rightarrow \infty) = D_{\text{move}}^{\text{FOG}}(k_z)} \quad (\text{D3})$$

The expression on $D_{\text{move}}^{\text{FOG}}$ can be further simplified. (1) Since \mathbf{v}_B is uncorrelated with \mathbf{v}_S and \mathbf{v}_S^s , we have $D_{\text{move}}^{\text{FOG}} = D_B^{\text{FOG}}(k_z) \langle e^{ik_z \Delta v_S/H} \rangle^2$. Here, $\Delta v_S \equiv v_{z,S} - v_{z,S}^s$. (2) So far we have neglected shot noise in the galaxy distribution. Since it does not correlate with other components, it only causes damping. This effect can be completely described by a damping function $D_{\text{shot}}^{\text{FOG}}(ku)$, the same as the case of \mathbf{v}_B . For brevity, we will not consider this measurement noise hereafter.

The impact of \mathbf{v}_S^s is harder to deal with, largely due to correlation between \mathbf{v}_S and \mathbf{v}_S^s . To see their correlation, let us check the limit $k \rightarrow 0$. Now we have $\delta^s \simeq \delta - \nabla_z v_z/H$, the starting point to derive the Kaiser formula. Since $\delta_s = (\delta - \nabla_z v_{z,\delta}/H) - \nabla_z v_{z,S}/H$, we obtain $\delta_S^s \simeq$

$-\nabla_z v_{z,S}/H$. Through the relation $\theta_S^s(\mathbf{k}) = \delta_S^s(\mathbf{k})W^s(\mathbf{k})$, we have $\mathbf{v}_S^s(\mathbf{k}) \simeq (\mathbf{v}_S(\mathbf{k}) \cdot \hat{\mathbf{k}})u^2W^s(\mathbf{k})\hat{\mathbf{k}}$. Notice that *the velocity field \mathbf{v}_S^s is statistically anisotropic*. Under this limit, \mathbf{v}_S^s is completely correlated with \mathbf{v}^s .

Due to this correlation, we can not calculate $\langle \dots \rangle^2$ separately for $v_{z,S}$ and $v_{z,S}^s$. Nevertheless, using the relation

$$1 + \epsilon_{\text{move}}(k_z, \mathbf{r}) = e^{k_z^2 \langle \Delta v_{1S} \Delta v_{2S} \rangle / H^2 + O(\Delta v_S^4)}, \quad (\text{D4})$$

we obtain

$$P_{\text{move}}(k, u) = [P_{\delta\delta}(k) + P_{\Delta v \Delta v}(k, u)u^4 + \dots] \times D_{\text{move}}^{\text{FOG}}(k_z). \quad (\text{D5})$$

Here, $P_{\Delta v \Delta v}(k, u)$ is the power spectrum of $\Delta \mathbf{v}_S \equiv \mathbf{v}_S - \mathbf{v}_S^s$. Due to the intrinsically anisotropic \mathbf{v}_S^s , $P_{\Delta v \Delta v}(\mathbf{k})$ is also anisotropic and depends on both k and u . At large scale limit,

$$\begin{aligned} P_{\Delta v \Delta v}(\mathbf{k}) &\simeq P_{\theta_S \theta_S}(k)(1 - u^2W^s(\mathbf{k}))^2 \\ &\simeq P_{\theta_S \theta_S}(k) \frac{1}{(1 + f\tilde{W}u^2)^2}. \end{aligned} \quad (\text{D6})$$

This results shows a generic property $P_{\Delta v \Delta v}(k, u)/P_{\delta\delta}(k) \rightarrow 0$ when $k \rightarrow 0$, since both \mathbf{v}_S and \mathbf{v}_S^s vanish at large scales. We propose that, by tuning W^s such that P_{move} follows a form like Eq. D5, we could obtain the correct W^s and hence the correct \mathbf{v}_δ field.

The above result is obtained in the large scale limit. The situation beyond this limit is too complicated to discuss analytically and will be postponed for future study. For the same reason, we still lack of a rigorous mathematical proof nor numerical verification for the above proposal. However, given its potential in reconstructing the 3D peculiar velocity in a less model dependent way, we hope to explore this possibility in future works.

-
- [1] Y. Zheng and et al. (2012), in preparation.
[2] J. C. Jackson, MNRAS **156**, 1P (1972).
[3] W. L. W. Sargent and E. L. Turner, ApJL **212**, L3 (1977).
[4] P. J. E. Peebles, *The large-scale structure of the universe* (1980).
[5] N. Kaiser, MNRAS **227**, 1 (1987).
[6] J. A. Peacock and S. J. Dodds, MNRAS **267**, 1020 (1994), arXiv:astro-ph/9311057.
[7] W. E. Ballinger, J. A. Peacock, and A. F. Heavens, MNRAS **282**, 877 (1996), arXiv:astro-ph/9605017.
[8] J. A. Peacock, S. Cole, P. Norberg, C. M. Baugh, J. Bland-Hawthorn, T. Bridges, R. D. Cannon, M. Colless, C. Collins, W. Couch, et al., Nature (London) **410**, 169 (2001), arXiv:astro-ph/0103143.
[9] M. Tegmark, A. J. S. Hamilton, and Y. Xu, MNRAS **335**, 887 (2002), arXiv:astro-ph/0111575.
[10] M. Tegmark, M. R. Blanton, M. A. Strauss, F. Hoyle, D. Schlegel, R. Scoccimarro, M. S. Vogeley, D. H. Weinberg, I. Zehavi, A. Berlind, et al., Astrophys. J. **606**, 702 (2004), arXiv:astro-ph/0310725.
[11] L. Samushia, W. J. Percival, and A. Raccanelli, MNRAS **420**, 2102 (2012), 1102.1014.
[12] L. Guzzo, M. Pierleoni, B. Meneux, E. Branchini, O. Le Fèvre, C. Marinoni, B. Garilli, J. Blaizot, G. De Lucia, A. Pollo, et al., Nature (London) **451**, 541 (2008), 0802.1944.
[13] C. Blake, S. Brough, M. Colless, C. Contreras, W. Couch, S. Croom, T. Davis, M. J. Drinkwater, K. Forster, D. Gilbank, et al., MNRAS **415**, 2876 (2011), 1104.2948.
[14] C. Blake, S. Brough, M. Colless, C. Contreras, W. Couch, S. Croom, D. Croton, T. Davis, M. J. Drinkwater, K. Forster, et al., ArXiv e-prints (2012), 1204.3674.
[15] B. A. Reid, L. Samushia, M. White, W. J. Percival, M. Manera, N. Padmanabhan, A. J. Ross, A. G. Sánchez, S. Bailey, D. Bizyaev, et al., ArXiv e-prints (2012),

- 1203.6641.
- [16] R. Tojeiro, W. J. Percival, J. Brinkmann, J. R. Brownstein, D. Eisenstein, M. Manera, C. Maraston, C. K. McBride, D. Duna, B. Reid, et al., ArXiv e-prints (2012), 1203.6565.
- [17] L. Amendola, C. Quercellini, and E. Giallongo, MNRAS **357**, 429 (2005), arXiv:astro-ph/0404599.
- [18] K. Yamamoto, B. A. Bassett, and H. Nishioka, Physical Review Letters **94**, 051301 (2005), arXiv:astro-ph/0409207.
- [19] Y. Wang, JCAP **5**, 21 (2008), 0710.3885.
- [20] W. J. Percival and M. White, MNRAS **393**, 297 (2009), 0808.0003.
- [21] Y.-S. Song and W. J. Percival, JCAP **10**, 4 (2009), 0807.0810.
- [22] M. White, Y.-S. Song, and W. J. Percival, MNRAS **397**, 1348 (2009), 0810.1518.
- [23] Y.-S. Song, Phys. Rev. D **83**, 103009 (2011), 1009.2753.
- [24] Y. Wang, W. Percival, A. Cimatti, P. Mukherjee, L. Guzzo, C. M. Baugh, C. Carbone, P. Franzetti, B. Garilli, J. E. Geach, et al., MNRAS **409**, 737 (2010), 1006.3517.
- [25] P. Zhang, M. Liguori, R. Bean, and S. Dodelson, Physical Review Letters **99**, 141302 (2007), 0704.1932.
- [26] B. Jain and P. Zhang, Phys. Rev. D **78**, 063503 (2008), 0709.2375.
- [27] E. V. Linder, Astroparticle Physics **29**, 336 (2008), 0709.1113.
- [28] R. Reyes, R. Mandelbaum, U. Seljak, T. Baldauf, J. E. Gunn, L. Lombriser, and R. E. Smith, Nature (London) **464**, 256 (2010), 1003.2185.
- [29] Y.-C. Cai and G. Bernstein, MNRAS **422**, 1045 (2012), 1112.4478.
- [30] E. Gaztañaga, M. Eriksen, M. Crocce, F. J. Castander, P. Fosalba, P. Marti, R. Miquel, and A. Cabré, MNRAS p. 2931 (2012), 1109.4852.
- [31] E. Jennings, C. M. Baugh, B. Li, G.-B. Zhao, and K. Koyama, ArXiv e-prints (2012), 1205.2698.
- [32] B. Li, W. A. Hellwing, K. Koyama, G.-B. Zhao, E. Jennings, and C. M. Baugh, ArXiv e-prints (2012), 1206.4317.
- [33] H.-J. Seo and D. J. Eisenstein, Astrophys. J. **598**, 720 (2003), arXiv:astro-ph/0307460.
- [34] D. J. Eisenstein, I. Zehavi, D. W. Hogg, R. Scoccimarro, M. R. Blanton, R. C. Nichol, R. Scranton, H.-J. Seo, M. Tegmark, Z. Zheng, et al., Astrophys. J. **633**, 560 (2005), arXiv:astro-ph/0501171.
- [35] C. Blake, E. A. Kazin, F. Beutler, T. M. Davis, D. Parkinson, S. Brough, M. Colless, C. Contreras, W. Couch, S. Croom, et al., MNRAS **418**, 1707 (2011), 1108.2635.
- [36] L. Anderson, E. Aubourg, S. Bailey, D. Bizyaev, M. Blanton, A. S. Bolton, J. Brinkmann, J. R. Brownstein, A. Burden, A. J. Cuesta, et al., ArXiv e-prints (2012), 1203.6594.
- [37] E. V. Linder, Phys. Rev. D **72**, 043529 (2005), arXiv:astro-ph/0507263.
- [38] D. Schlegel, F. Abdalla, T. Abraham, C. Ahn, C. Allende Prieto, J. Annis, E. Aubourg, M. Azzaro, S. B. C. Baltay, C. Baugh, et al., ArXiv e-prints (2011), 1106.1706.
- [39] R. Laureijs, J. Amiaux, S. Arduini, J. . Auguères, J. Brinchmann, R. Cole, M. Cropper, C. Dabin, L. Duvet, A. Ealet, et al., ArXiv e-prints (2011), 1110.3193.
- [40] U.-L. Pen, Astrophys. J. **504**, 601 (1998), arXiv:astro-ph/9711180.
- [41] Y. P. Jing, H. J. Mo, and G. Boerner, Astrophys. J. **494**, 1 (1998), arXiv:astro-ph/9707106.
- [42] R. Scoccimarro, Phys. Rev. D **70**, 083007 (2004), arXiv:astro-ph/0407214.
- [43] U. Seljak and P. McDonald, JCAP **11**, 39 (2011), 1109.1888.
- [44] T. Okumura, U. Seljak, P. McDonald, and V. Desjacques, JCAP **2**, 10 (2012), 1109.1609.
- [45] T. Okumura, U. Seljak, and V. Desjacques, ArXiv e-prints (2012), 1206.4070.
- [46] S. Bonoli and U. L. Pen, MNRAS **396**, 1610 (2009), 0810.0273.
- [47] V. Desjacques and R. K. Sheth, Phys. Rev. D **81**, 023526 (2010), 0909.4544.
- [48] A. J. S. Hamilton and M. Culhane, MNRAS **278**, 73 (1996), arXiv:astro-ph/9507021.
- [49] X. Kang, Y. P. Jing, H. J. Mo, and G. Börner, MNRAS **336**, 892 (2002), arXiv:astro-ph/0201124.
- [50] A. F. Heavens, S. Matarrese, and L. Verde, MNRAS **301**, 797 (1998), arXiv:astro-ph/9808016.
- [51] T. Matsubara, Phys. Rev. D **77**, 063530 (2008), 0711.2521.
- [52] T. Matsubara, Phys. Rev. D **78**, 083519 (2008), 0807.1733.
- [53] A. Taruya, T. Nishimichi, and S. Saito, Phys. Rev. D **82**, 063522 (2010), 1006.0699.
- [54] T. Matsubara, Phys. Rev. D **83**, 083518 (2011), 1102.4619.
- [55] T. Okamura, A. Taruya, and T. Matsubara, JCAP **8**, 12 (2011), 1105.1491.
- [56] M. Sato and T. Matsubara, Phys. Rev. D **84**, 043501 (2011), 1105.5007.
- [57] M. White, MNRAS **321**, 1 (2001), arXiv:astro-ph/0005085.
- [58] U. Seljak, MNRAS **325**, 1359 (2001), arXiv:astro-ph/0009016.
- [59] J. L. Tinker, D. H. Weinberg, and Z. Zheng, MNRAS **368**, 85 (2006), arXiv:astro-ph/0501029.
- [60] J. L. Tinker, MNRAS **374**, 477 (2007), arXiv:astro-ph/0604217.
- [61] K. B. Fisher, Astrophys. J. **448**, 494 (1995), arXiv:astro-ph/9412081.
- [62] B. A. Reid and M. White, MNRAS **417**, 1913 (2011), 1105.4165.
- [63] T. Okumura and Y. P. Jing, Astrophys. J. **726**, 5 (2011), 1004.3548.
- [64] E. Jennings, C. M. Baugh, and S. Pascoli, MNRAS **410**, 2081 (2011), 1003.4282.
- [65] J. Kwan, G. F. Lewis, and E. V. Linder, Astrophys. J. **748**, 78 (2012), 1105.1194.
- [66] E. Jennings, C. M. Baugh, and S. Pascoli, ApJL **727**, L9 (2011), 1011.2842.
- [67] D. Bianchi, L. Guzzo, E. Branchini, E. Majerotto, S. de la Torre, F. Marulli, L. Moscardini, and R. E. Angulo, ArXiv e-prints (2012), 1203.1545.
- [68] S. de la Torre and L. Guzzo, ArXiv e-prints (2012), 1202.5559.
- [69] F. Bernardeau, S. Colombi, E. Gaztañaga, and R. Scoccimarro, Physics reports **367**, 1 (2002), arXiv:astro-ph/0112551.
- [70] S. Pueblas and R. Scoccimarro, Phys. Rev. D **80**, 043504 (2009), 0809.4606.
- [71] B. Jain and J. Khoury, Annals of Physics **325**, 1479

- (2010), 1004.3294.
- [72] T. Clifton, P. G. Ferreira, A. Padilla, and C. Skordis, *Physics reports* **513**, 1 (2012), 1106.2476.
 - [73] A. Cooray and R. Sheth, *Physics reports* **372**, 1 (2002), arXiv:astro-ph/0206508.
 - [74] X. Yang, H. J. Mo, and F. C. van den Bosch, *MNRAS* **339**, 1057 (2003), arXiv:astro-ph/0207019.
 - [75] Z. Zheng, A. A. Berlind, D. H. Weinberg, A. J. Benson, C. M. Baugh, S. Cole, R. Davé, C. S. Frenk, N. Katz, and C. G. Lacey, *Astrophys. J.* **633**, 791 (2005), arXiv:astro-ph/0408564.
 - [76] T. Hamana, I. Kayo, N. Yoshida, Y. Suto, and Y. P. Jing, *MNRAS* **343**, 1312 (2003), arXiv:astro-ph/0305187.
 - [77] R. K. Sheth and A. Diaferio, *MNRAS* **322**, 901 (2001), arXiv:astro-ph/0009166.
 - [78] L. Lombriser, *Phys. Rev. D* **83**, 063519 (2011), 1101.0594.
 - [79] S. Ho, S. Dedeo, and D. Spergel, *ArXiv e-prints* (2009), 0903.2845.
 - [80] J. Shao, P. Zhang, W. Lin, Y. Jing, and J. Pan, *MNRAS* **413**, 628 (2011), 1004.1301.
 - [81] R. A. Sunyaev and I. B. Zeldovich, *MNRAS* **190**, 413 (1980).
 - [82] J. Dunkley, R. Hlozek, J. Sievers, V. Acquaviva, P. A. R. Ade, P. Aguirre, M. Amiri, J. W. Appel, L. F. Barrientos, E. S. Battistelli, et al., *Astrophys. J.* **739**, 52 (2011), 1009.0866.
 - [83] N. Hand, G. E. Addison, E. Aubourg, N. Battaglia, E. S. Battistelli, D. Bizyaev, J. R. Bond, H. Brewington, J. Brinkmann, B. R. Brown, et al., *ArXiv e-prints* (2012), 1203.4219.
 - [84] E. Shirokoff, C. L. Reichardt, L. Shaw, M. Millea, P. A. R. Ade, K. A. Aird, B. A. Benson, L. E. Bleem, J. E. Carlstrom, C. L. Chang, et al., *Astrophys. J.* **736**, 61 (2011), 1012.4788.
 - [85] C. L. Reichardt, L. Shaw, O. Zahn, K. A. Aird, B. A. Benson, L. E. Bleem, J. E. Carlstrom, C. L. Chang, H. M. Cho, T. M. Crawford, et al., *ArXiv e-prints* (2011), 1111.0932.
 - [86] In reality, some k modes of $W(k)$ and $P_{\theta_S\theta_S}(k)$ may not be well constrained to provide sufficiently accurate prediction on σ_{v_δ} or σ_{v_S} . In this case, we may need to treat σ_{v_δ} and σ_{v_S} as free parameters.